Chapter 7

Interaction with human serum albumin:

Fluorescence and phosphorescence study for racemic brompheniramine

S. Tardioli*, I. Lammers*, J.-H. Hooijschuur, F. Ariese, G. van der Zwan, and C. Gooijer
(*contributed equally) *Submitted for publication*

Abstract

Binding of the antihistamine drug brompheniramine (BPA) to human serum albumin (HSA) is studied by measuring the quenching of the fluorescence and room-temperature phosphorescence (RTP) of the single tryptophan of this protein. The modified Stern-Volmer equation was used to derive association constants and accessible fractions from the steady-state fluorescence data. Decay-associated spectra (DAS) revealed three tryptophan fluorescence lifetimes with different fluorescence maxima, indicating the presence of several HSA conformations. BPA causes mainly static fluorescence quenching of the long-living, solvent-exposed conformer. RTP spectra and lifetimes, recorded under deoxygenated conditions in the presence of 0.2 M KI, provided additional kinetic information about the interaction between HSA and BPA. For comparison of the fluorescence and phosphorescence data, fluorescence DAS were also recorded in the presence of 0.2 M KI and revealed that the solvent-exposed conformer is the major contributor to the RTP signal. The phosphorescence quenching is mostly dynamic at pH 7 and mostly static at pH 9, presumably related to the protonation state of the alkylamino chain of BPA.

7.1 Introduction

Binding of drugs to the transport protein human serum albumin (HSA) has been the subject of a large number of investigations. [1-3] A wide variety of techniques has been applied for this purpose, based on separation methods on the one hand and spectroscopic methods on the other, with focus on binding constants. For instance, Martínez-Gómez and coworkers studied the binding of antihistamines[4] and other drugs[5] by monitoring the mobility in capillary electrophoresis. Yoo *et al.*[6] used the chromatographic behavior in HSA-packed microcolumns to determine overall drug binding constants. Chadborn *et al.*[7] used tryptophan fluorescence quenching to study drug-induced conformational changes in albumins. However, it is still challenging to interpret these binding constants since various binding sites of HSA are available.[8] For pharmacokinetic modeling, the results of such studies should preferably be combined with information about the dynamics.

HSA contains only a single tryptophan and this amino acid is situated near a primary binding site. Therefore, fluorescence spectroscopy at selective wavelengths can provide direct information about interactions in case the ligand binding influences the tryptophan luminescence properties. Unfortunately, as is well known from the literature,[9] even proteins with a single tryptophan residue often show more than a single fluorescence lifetime, which can be attributed to the existence of multiple protein conformations. This is also the case for HSA. Since nearby amino acid residues can act as quenchers of tryptophan fluorescence, even slightly different protein conformations can result in different decay times. The longest lifetime (as long as 7 ns) of single-tryptophan proteins is usually observed at the red side of the emission spectrum and is attributed to water-exposed tryptophan residues. Buried tryptophans often show shorter lifetimes as a result of the above mentioned quenching effects.[9]

For fluorescence quenching of proteins with more than one tryptophan, non-linear Stern-Volmer plots are obtained when the individual fluorophores are not equally accessible to the quencher.[10,11] For the investigation of the quenching processes of such proteins, a modified Stern-Volmer equation has to be used

$$\frac{F_0}{F_0 - F} = \frac{1}{f_a \cdot K_a \cdot [Q]} + \frac{1}{f_a} \qquad \textbf{Eq. 7.1}$$

where F_0 and F represent the fluorescence intensities of the protein in absence and in presence of quencher, respectively, and $[Q]$ is the quencher concentration.[9] From a plot of $F_0/(F_0\text{-}F)$ versus $[Q]^{-1}$, the values of the fraction of accessible tryptophans f_a (1/intercept) and the quencher association constant K_a (1/(f_a×slope)) can be obtained. The question needs to be addressed whether in the case of HSA, which only contains a single tryptophan but is present in more conformations, differences in accessibility also play a role. Static fluorescence

quenching experiments of HSA with the antihistamine compound chlorpheniramine seem to suggest this.[12]

The tryptophan moiety in proteins is not only fluorescent but can also emit phosphorescence at room temperature (RTP).[13] RTP of HSA under liquid conditions is not easily detected, but Wei and coworkers[14] showed that intense phosphorescence spectra can be obtained if the samples are deoxygenated and KI is added as heavy atom reagent. Phosphorescence can provide valuable information about protein structure and dynamics in the micro- to millisecond regime, in contrast to fluorescence phenomena, which take place on a nanosecond timescale. Proteins with a single tryptophan residue may show more than a single phosphorescence lifetime, indicating the presence of multiple conformations that are stable at the phosphorescence timescale.[15,16]

Brompheniramine (BPA; Figure 7.1) is a chiral antihistaminic drug with a pK_a of 9.1; at neutral pH the fraction of deprotonated BPA is negligible, whereas at pH 9.0 it is close to 50%.[17] Binding to HSA can be influenced by the charge of the BPA tail, and therefore the equilibrium constant is expected to be pH dependent. As far as we know, for the interaction of BPA and HSA only the overall binding constant has been determined. Martínez-Gómez and coworkers[4] determined the fraction of unbound drug at various HSA levels in a capillary electrophoresis setup at pH 7.4 and derived an association constant of $(1.8\pm0.3)\times10^3$ M^{-1} assuming that there is only a single independent binding site involved.

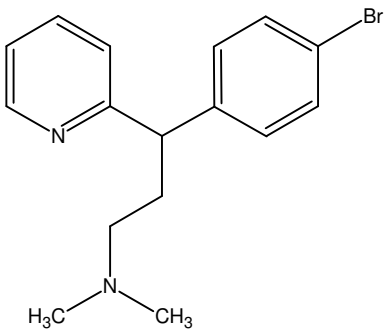

Figure 7.1: Molecular structure of brompheniramine.

In the present chapter, the binding of HSA and BPA is investigated at pH 7 and pH 9 based on quenching of the HSA luminescence. In addition to steady-state fluorescence, also time-resolved fluorescence is used to study the quenching phenomena in more detail based on decay-associated spectra (DAS). Complementary phosphorescence information will be obtained in the spectral as well as in the time domain to gain additional insight into association constants as well as into binding kinetics.

7.2 Experimental section

7.2.1 Chemicals

Fatty acid free albumin from human serum (≥ 96%), L-tryptophan, (±)-brompheniramine maleate salt, boric acid, potassium iodide and sodium sulfite were purchased from Sigma-Aldrich (St. Louis, MO, USA); unfortunately, to the best of our knowledge, the separate enantiomers of BPA were not commercially available. Sodium hydroxide was from Fluka (Buchs, Switzerland). Potassium dihydrogen phosphate and potassium monohydrogen phosphate were obtained from J.T. Baker (Deventer, the Netherlands). All chemicals were used as received. Water was purified with a Milli-Q system from Millipore (Bedford, MA, USA).

7.2.2 Fluorescence

Fluorescence emission spectra were recorded at room temperature on a LS50B spectrometer, using a square quartz cuvette of 10-mm path length. All measurements were performed at an excitation wavelength of 295 nm and spectral band widths of 10 nm. Static fluorescence spectra of HSA and BPA mixtures were determined in 10 mM phosphate buffer (pH 7.2) or 10 mM borate buffer (pH 9.0) at a fixed protein concentration of 4 mM and varying BPA concentrations of 0.10, 0.27, 0.61, and 1.63 mM. The emission at 350 nm was used to construct Stern-Volmer plots.

Time-correlated single-photon counting (TCSPC) was used to determine fluorescence intensity decays. The excitation source was a Ti:Sapph laser (Coherent, Mira 900, Santa Clara, CA, USA) with a pulse width of 3 ps. A pulse picker was used to reduce the laser repetition rate to 4 MHz. The output of the laser was frequency tripled to get an excitation wavelength of 295 nm. A multichannel-plate photomultiplier (Hamamatsu, R3809U-50, Japan) collected the fluorescence emission, and data were recorded by a SPC-630 module (Becker & Hickl GmbH, Berlin, Germany) with a time resolution of 15 ps. Fluorescence decay curves were analyzed using a global fitting procedure based on the Levenberg-Marquardt algorithm. The instrument response function (determined by collecting scattered light from a suspension of silica particles) was used for deconvolution of the recorded decays and for determination of lifetimes and wavelength-dependent amplitudes. Each intensity curve was fitted with a multi-exponential decay, and the goodness of the fit was assessed on the basis of χ^2 and the distribution of residuals.

The decay-associated spectra (DAS) were constructed by distributing the total intensity per decay curve over the lifetimes that make up the total intensity according to their amplitudes obtained by the above fit procedure. The relative fluorescence intensity $I_j(\lambda)$ of a lifetime component (τ_j) with amplitude (A_j) at a certain wavelength (λ) can be expressed by Equation 7.2:

$$I_j(\lambda) = \frac{A_j(\lambda)\tau_j}{\sum_i A_i(\lambda)\tau_i} \qquad \textbf{Eq. 7.2}$$

The sum in the denominator of this expression is equal to the steady-state emission spectrum.

7.2.3 Phosphorescence

A Cary Eclipse luminescence spectrometer (Varian, Melbourne, Australia) was used to record the HSA phosphorescence. For enhancing the phosphorescence emission, 0.2 M KI was used in each sample. Chemical deoxygenation was achieved by adding 2 mM Na_2SO_3 just before capping the 10-mm square quartz cuvettes. The temperature was kept at 20°C using the single-cell Peltier cooler of the spectrometer. The phosphorescence emission spectra were recorded with an excitation wavelength of 290 nm, spectral band widths of 10 nm, a delay time of 0.1 ms, and a total gate time of 5 ms. The intensities were corrected for the signal loss during the delay time by multiplication with a correction factor depending on the phosphorescence lifetimes. Time-resolved phosphorescence decay curves were obtained for the determination of lifetimes with an excitation wavelength of 290 nm, an emission wavelength of 443 nm, spectral band widths of 10 nm, an initial delay of 50 µs, a gate width of 50 µs, and a total decay time of 15 ms. OriginPro 8.0 was used to fit the phosphorescence decay curves with a bi-exponential decay function, and the goodness of the fit was assessed on the basis of χ^2 and the distribution of residuals.

7.3 Results and discussion

7.3.1 Fluorescence

In this subsection on HSA tryptophan fluorescence, static and time-resolved data on the quenching of 4 mM HSA by various concentrations of BPA (0-1.63 mM) will be presented at pH 7.2 and at pH 9.0. In order to couple the fluorescence with the phosphorescence results, the effect of adding KI on the HSA fluorescence was investigated as well. Tryptophan was selectively excited at 295 nm; other amino acid residues and BPA do not absorb at this wavelength.

When plotting the steady-state quenching data using the regular Stern-Volmer equation, no linear relationship was obtained. Such behavior may be caused by differences in accessibility of the tryptophan due to different protein conformations present in solution. Indeed, at both pH values linear plots were obtained with the modified Stern-Volmer relationship (data not shown). The steady-state fluorescence experiments showed a clear pH dependence: an equilibrium binding constant of $(2.2\pm0.3)\times10^3$ M^{-1} with $f_a = 0.50\pm0.03$ was determined at pH 7.2, while a binding constant of $(9.1\pm2.2)\times10^3$ M^{-1} with $f_a = 0.71\pm0.03$ was obtained at pH 9.0. The protonated ligand at pH 7.2 has a lower association constant,

which may indicate a non-polar binding mechanism. Note that the binding constant of $(2.2\pm0.3)\times10^3$ M^{-1} determined at pH 7.2 corresponds well with the value of $(1.8\pm0.3)\times10^3$ M^{-1} reported by Martínez-Gómez *et al.*[4] at pH 7.4. It should be realized that the latter value refers to the overall BPA-HSA binding, whereas the association constants derived from the Stern-Volmer plots refer only to binding modes that affect the fluorescence quantum yield. Apparently, in the case of BPA other non-quenching binding modes do not play a major role.

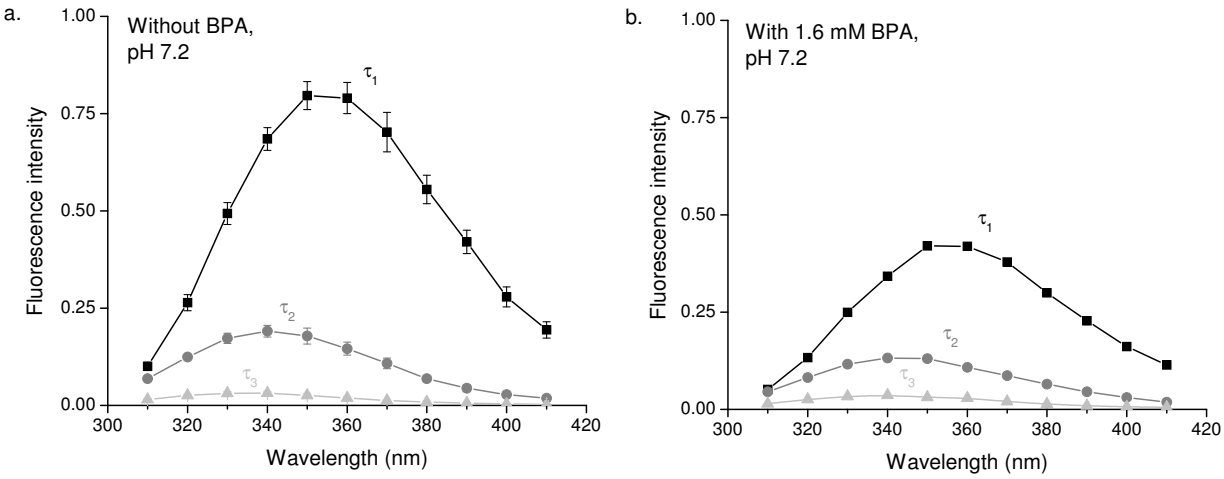

Figure 7.2: Decay-associated fluorescence emission spectra of 4 µM HSA at pH 7.2 (a) in absence of BPA with lifetimes τ_1 = 7.2 ns (■), τ_2 = 2.6 ns (●), and τ_3 = 0.4 ns (▲) and (b) in presence of 1.6 mM BPA with lifetimes τ_1 = 6.9 ns (■), τ_2 = 2.6 ns (●), and τ_3 = 0.4 ns (▲). Samples were made in 10 mM phosphate buffer. Laser excitation was performed at 295 nm. The total intensity of (a) is normalized to 1 and (b) is on the same scale.

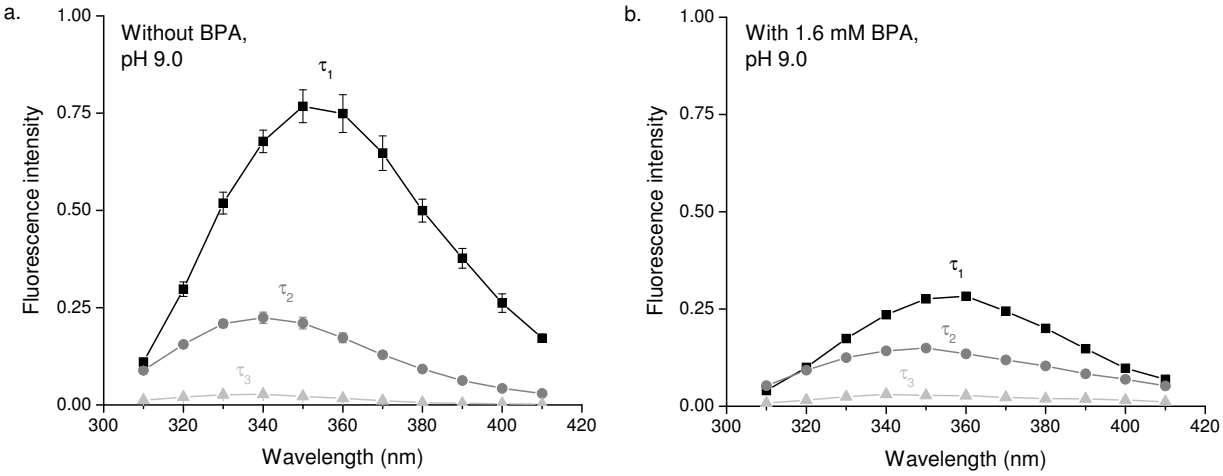

Figure 7.3: Decay-associated fluorescence emission spectra of 4 µM HSA at pH 9.0 (a) in absence of BPA with lifetimes τ_1 = 6.7 ns (■), τ_2 = 2.6 ns (●), and τ_3 = 0.4 ns (▲) and (b) in presence of 1.6 mM BPA with lifetimes τ_1 = 5.8 ns (■), τ_2 = 2.6 ns (●), and τ_3 = 0.4 ns (▲). Samples were made in 10 mM borate buffer. Laser excitation was performed at 295 nm. The total intensity of (a) is normalized to 1 and (b) is on the same scale.

Time-resolved fluorescence experiments were performed in order to study the binding in more detail. The DAS of HSA in the absence of BPA and in the presence of 1.63 mM BPA are shown in Figure 7.2 for pH 7.2 and in Figure 7.3 for pH 9.0. Three fluorescence lifetimes

of 7.2, 2.6, and 0.4 ns are obtained without quencher at pH 7.2. Similar lifetimes of 6.7, 2.6, and 0.4 ns are found at pH 9.0. Apparently, the protein does not undergo major conformational changes that involve the direct environment of the tryptophan moiety over the pH range from 7.2 to 9.0 on the fluorescence timescale. This is in line with the findings of Amari *et al.*[18] and of Otosu *et al.*[19], who noted that the tryptophan lifetimes change significantly only at more extreme pH values.

The DAS corresponding to the three HSA fluorescence lifetimes (Figures 7.2a and 7.3a) are different: the maximum wavelength of the 7.2/6.7 ns fluorescence is about 355 nm, some 15 nm red-shifted in comparison with that of the shorter-living species. This is in accordance with other single-tryptophan proteins as discussed by Lakowicz.[9] In the following, these lifetimes will be equated with three different species, which will be referred to as conformers I, II and III. The longer living component (conformer I) is found at longer emission wavelengths, indicating that it is exposed to a more polar environment, possibly water, whereas tryptophan residues buried inside the protein matrix (conformers II and III) have shorter lifetimes and emit at shorter wavelengths. As indicated by the intensities in Figures 7.2a and 7.3a, the overall static HSA fluorescence spectrum is dominated by conformation I, in which the tryptophan is most exposed to quenching.

Time-resolved fluorescence quenching by BPA was studied over the concentration range from 0.10 to 1.63 mM BPA. The DAS at the highest BPA concentration are depicted in Figures 7.2b and 7.3b. Interestingly, the tryptophan fluorescence lifetimes are only little influenced by BPA addition: the longest lifetime is reduced from 7.2 to 6.9 ns (4%) at pH 7.2 and from 6.7 to 5.8 ns (15%) at pH 9.0. In other words, dynamic quenching of fluorescence plays only a negligible role at the BPA concentrations dealt with in this study. The DAS spectra in Figures 7.2 and 7.3 indicate a predominant intensity decrease of the long lifetime component. Therefore, the main cause of HSA fluorescence quenching is the static quenching of the tryptophan fluorescence of conformer I, while the contributions of conformers II and III are much less affected. This agrees with the hypothesis that multiple conformations with different tryptophan accessibilities exist, and supports the use of the modified Stern-Volmer equation for the steady-state quenching data. Similar results were obtained at an excitation wavelength of 288 nm (close to the absorption maximum of HSA) instead of 295 nm (red edge), confirming that the observed changes are not due to different spectral shifts of the tryptophan absorption band in the different HSA conformers upon binding (data not shown).

Sensitive room-temperature phosphorescence measurements require the presence of KI. In proteins containing several tryptophan residues, iodide is known to quench the fluorescence of only the solvent-exposed tryptophan moieties.[20] Therefore, we determined the effect of KI on the fluorescence characteristics of HSA. Figure 7.4 shows the DAS of HSA in absence and presence of 0.2 M KI at pH 7.2. Similar results were obtained at pH 9.0 (data not shown). Also in the presence of 0.2 M KI three lifetimes are observed, which are significantly shorter than the corresponding lifetimes in absence of KI. At pH 7.2, the longest lifetime

decreases from 7.2 to 4.6 ns (36%) and the second one from 2.6 to 1.8 ns (31%). Similarly, at pH 9.0, the longest lifetime decreases from 6.7 to 4.5 ns (33%) and the second one from 2.6 to 1.7 ns (35%). Because of the poorer precision, changes in the shortest lifetime of 0.3 ns are not taken into consideration. These lifetime changes indicate that iodide causes a similar degree of dynamic quenching for conformer I and II. The bimolecular rate constant for fluorescence quenching by iodide (k^+) can be calculated from the lifetime changes: for conformer I it is about 4×10^8 $M^{-1}s^{-1}$, and for conformer II it is even somewhat higher at 9×10^8 $M^{-1}s^{-1}$. Presumably, the heavy atom iodide species - through collisional interaction with tryptophan - causes an enhanced intersystem crossing rate from the first excited singlet state S_1 to the triplet state T_1, and thus a reduction in fluorescence lifetime.

The addition of 0.2 M KI reduces the fluorescence intensity of conformer I with a factor of 4 (Figure 7.4), which cannot completely be attributed to the lifetime decrease. Apparently, in addition to dynamic quenching also static quenching due to complex formation plays a role; the corresponding equilibrium association constant was calculated to be about $K = 8$ M^{-1}. Association of iodide with conformer II is of minor importance. The lifetime of the complex between HSA conformer I and iodide can be estimated, since $K = k^+/k^-$ where k^+ is the association rate and k^- is the dissociation rate of the complex. Using the values described above we get $k^- = 5\times10^7$ s^{-1}, and thus a lifetime of the complex of about 20 ns. Obviously, this is very short compared to the phosphorescence phenomena to be discussed below.

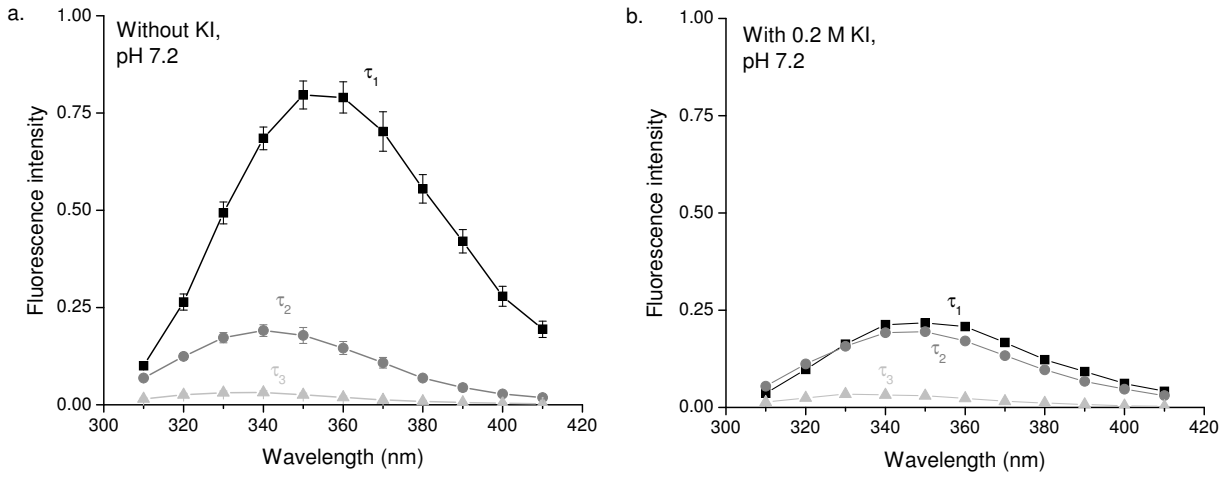

Figure 7.4: Decay-associated fluorescence emission spectra of 4 μM HSA at pH 7.2 (a) in absence of KI with lifetimes τ_1 = 7.2 ns (■), τ_2 = 2.6 ns (●), and τ_3 = 0.4 ns (▲) and (b) in presence of 0.2 M KI with lifetimes τ_1 = 4.6 ns (■), τ_2 = 1.8 ns (●), and τ_3 = 0.3 ns (▲). Samples were made in 10 mM phosphate buffer. Laser excitation was performed at 295 nm. The total intensity of (a) is normalized to 1 and (b) is on the same scale.

7.3.2 Phosphorescence

Following the fluorescence experiments, we also studied the static and dynamic effects of BPA on the HSA tryptophan phosphorescence. All samples were chemically deoxygenated to prevent the quenching of phosphorescence by dissolved oxygen.

Furthermore, 0.2 M KI was added to increase the phosphorescence luminescence by accelerating intersystem crossing processes. In addition, we will compare the HSA phosphorescence quenching with that of the free amino acid tryptophan. Contrary to the mono-exponential phosphorescence decay of free tryptophan (see below), HSA shows at least two phosphorescence lifetimes. The observation of several lifetimes for a protein with a single tryptophan indicates that conformational heterogeneity exists at the timescale of the phosphorescence emission.[15,16] This cannot be directly compared with the different conformers observed in fluorescence, since different timescales and different quenching mechanisms play a role. The time-resolved fluorescence experiments described above indicated that mainly conformer I with the more solvent-exposed tryptophan will contribute to the phosphorescence signal.

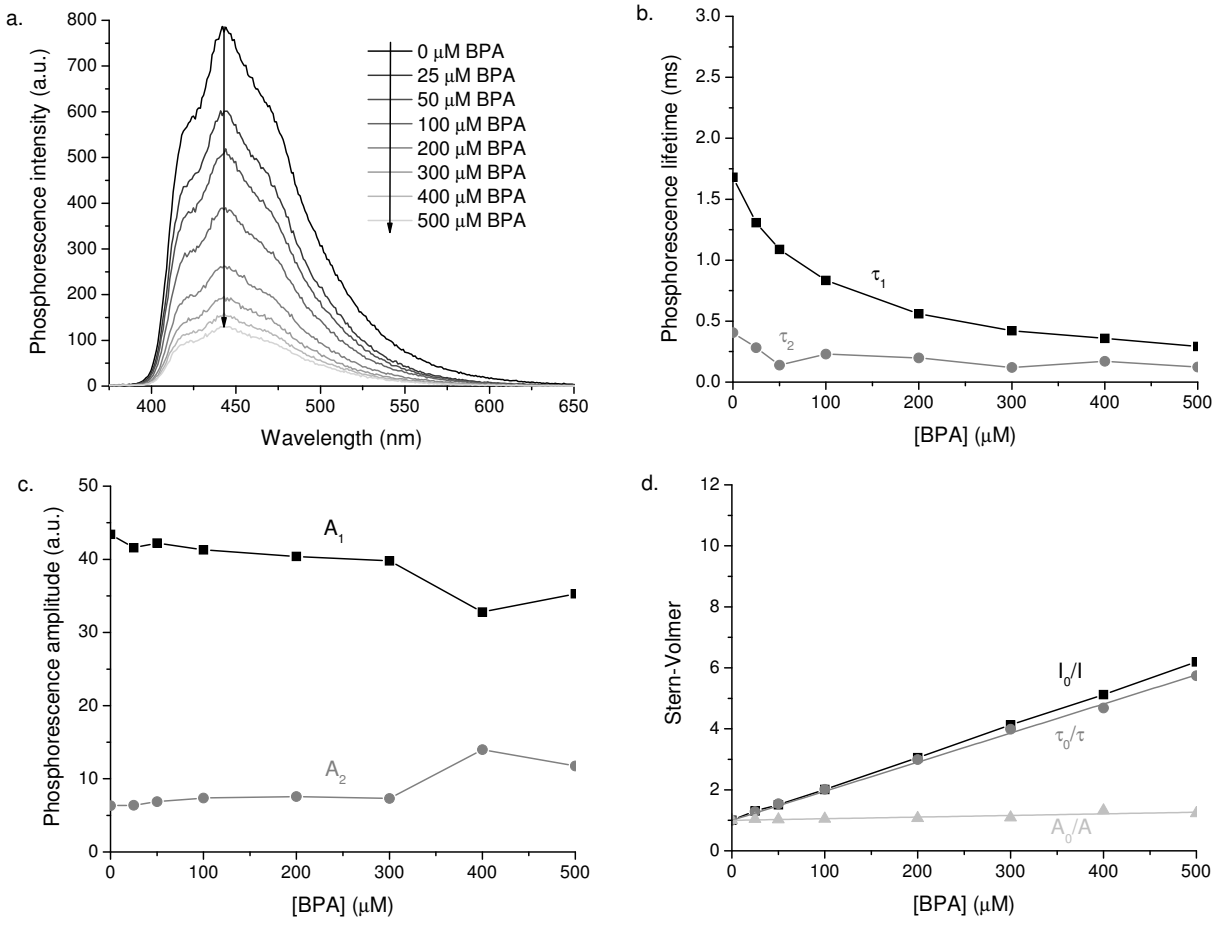

Figure 7.5: The influence of increasing BPA concentrations on the phosphorescence emission of 4 μM HSA at pH 7.0: (a) phosphorescence emission spectra, (b) phosphorescence lifetimes τ_1 (■) and τ_2 (●) with (c) their corresponding amplitudes A_1 (■) and A_2 (●), and (d) Stern-Volmer plots based on the overall intensity I_0/I (■), the longest lifetime τ/τ_0 (●), and its corresponding amplitude A_0/A (▲). All samples contained 10 mM phosphate buffer, 0.2 M KI to enhance the intersystem crossing, and 2 mM Na_2SO_3 for deoxygenation. Excitation at 290 nm was performed with a xenon lamp.

Figure 7.5a shows the RTP spectra of 4 μM HSA in the presence of BPA concentrations ranging from 0 to 500 μM. The HSA tryptophan phosphorescence is strongly quenched by BPA and the corresponding Stern-Volmer plot I_0/I is shown in Figure 7.5d. In order to evaluate the nature of the quenching mechanism, the phosphorescence lifetimes and associated amplitudes as a function of the BPA concentration are shown in Figures 7.5b and 7.5c, respectively. A decrease in phosphorescence lifetime indicates a process occurring during the lifetime of the excited triplet state (dynamic quenching), whereas a decrease in amplitude indicates the formation of a non-phosphorescent complex (static quenching). At pH 7.0 in absence of BPA, two phosphorescence lifetimes of 1.7 ms and 0.4 ms are found with relative amplitudes of 6:1. Upon addition of BPA, the lifetime of the long-living conformer strongly decreases in agreement with a species in which the tryptophan is relatively accessible. The amplitude of this species hardly changes upon adding BPA; apparently the phosphorescence quenching mechanism at pH 7.0 is mainly dynamic. The Stern-Volmer plot τ_0/τ for the long-lifetime component shows a linear relationship with the BPA concentration, which corresponds with a rate constant of dynamic quenching of $(5.7\pm0.2)\times10^6$ M^{-1} s^{-1} (Figure 7.5d). Although the associated amplitude change is minor and cannot be determined very precisely, a binding constant of $(5.3\pm3.0)\times10^2$ M^{-1} was calculated from the Stern-Volmer plot A_0/A (Figure 7.5d). This is reasonably close to the binding constant derived from the static fluorescence experiments described in the previous section ($(2.2\pm0.3)\times10^3$ M^{-1}).

The RTP results at pH 9.0 are quite different from those at neutral pH, as can be seen in Figure 7.6. Again, two lifetimes are found; the long-living component has a longer lifetime (2.6 ms) and a lower amplitude than at pH 7.0, whereas the short-living component has a slightly shorter lifetime (0.3 ms) and a distinctly higher amplitude than at pH 7.0. By plotting τ_0/τ for the long lifetime component as a function of the BPA concentration (Figure 7.6d) a linear curve is obtained with a dynamic quenching constant of $(1.3\pm0.1)\times10^6$ M^{-1} s^{-1}, which is 4 to 5 times lower than at pH 7.0. In contrast to the results obtained under neutral conditions, the phosphorescence of the long-living conformer does not only undergo dynamic quenching but also significant static quenching at pH 9.0. The formation of a non-phosphorescent complex is evident from Figure 7.6c, which shows a strong decrease in amplitude A_1 at higher BPA levels. From the Stern-Volmer plot A_0/A based on the amplitude of the long-living conformer (Figure 7.6d), the association constant was calculated to be $(1.6\pm0.1)\times10^4$ M^{-1}. Again, this value is quite close to that found with the static fluorescence quenching experiments described above ($(9.1\pm2.2)\times10^3$ M^{-1}) and confirms the stronger binding of BPA to HSA at higher pH.

In a separate set of experiments, we studied the quenching effect of BPA on the phosphorescence of the amino acid tryptophan in deoxygenated solutions in the presence of 0.2 M KI. Both at pH 7.0 and 9.0, dynamic quenching rates of free tryptophan by BPA of about 1×10^9 M^{-1} were obtained, which is close to the diffusion-controlled rate constant (data not shown). The rate constants of dynamic quenching for HSA are 2-3 orders of magnitude

lower than those for free tryptophan, in line with a reduced accessibility of the tryptophan moiety in the protein.

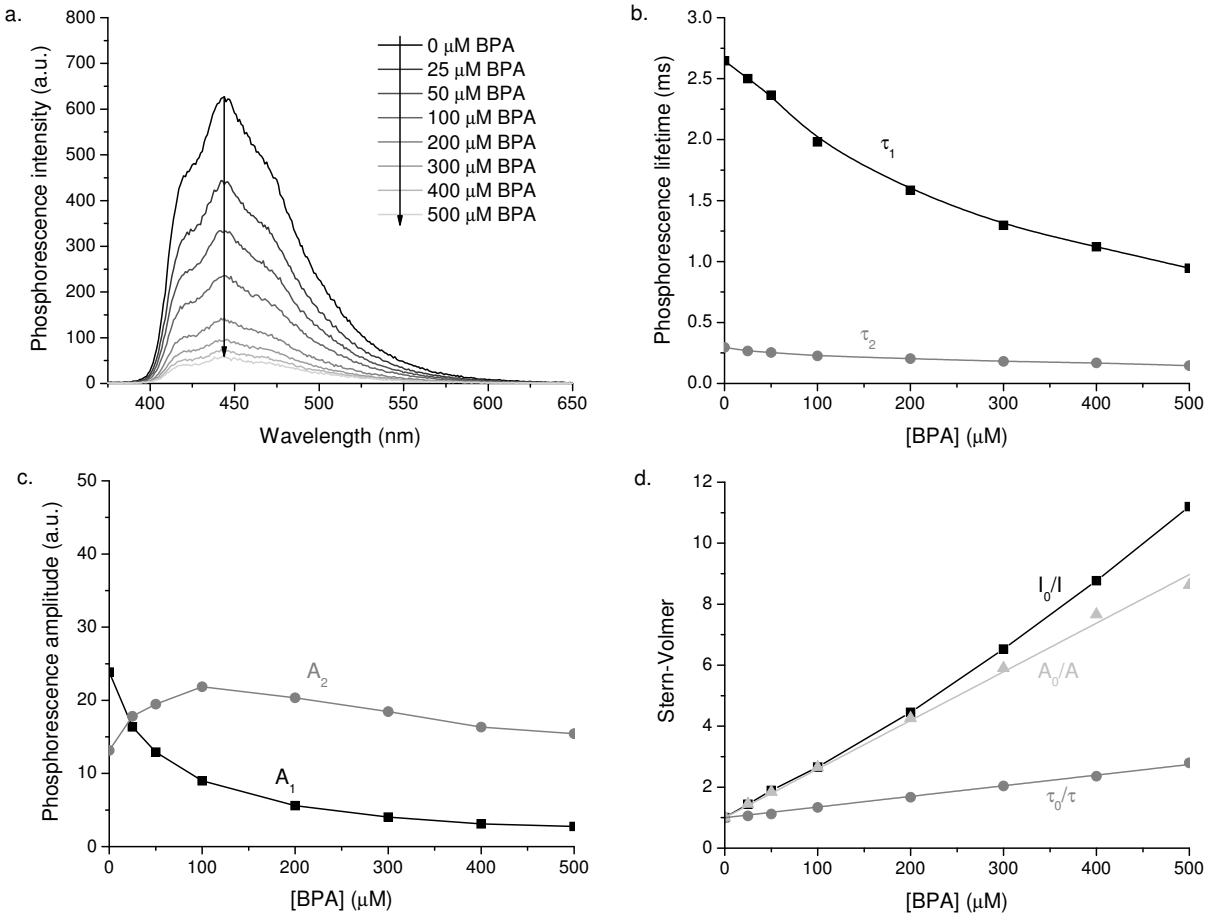

Figure 7.6: The influence of increasing BPA concentrations on the phosphorescence emission of 4 μM HSA at pH 9.0: (a) phosphorescence emission spectra, (b) phosphorescence lifetimes τ_1 (■) and τ_2 (●) with (c) their corresponding amplitudes A_1 (■) and A_2 (●), and (d) Stern-Volmer plots based on the overall intensity I_0/I (■), the longest lifetime τ_0/τ (●), and its corresponding amplitude A_0/A (▲). All samples contained 10 mM borate buffer, 0.2 M KI to enhance the intersystem crossing, and 2 mM Na_2SO_3 for deoxygenation. Excitation at 290 nm was performed with a xenon lamp.

7.4 Conclusions

Despite the fact that HSA is a single-tryptophan protein, modeling of steady-state tryptophan fluorescence quenching of HSA by BPA required the use of the modified Stern-Volmer equation, indicating the existence of tryptophans with a different accessibility for quenchers. Fluorescence decay-associated spectra showed that the three HSA fluorescence lifetimes are associated with different emission spectra, which indicates the presence of several HSA conformers. Mainly the more exposed tryptophan of conformer I is amenable to static fluorescence quenching upon addition of BPA, whereas the quenching of conformers II and III is less pronounced. The heavy-atom induced phosphorescence of HSA is dominated by the tryptophan moiety in conformer I interacting with iodide. Both the fluorescence and the

phosphorescence quenching experiments showed a stronger binding at higher pH, presumably related to the deprotonated (less polar) state of the alkylamino chain. Not only association constants can be derived from time-resolved phosphorescence measurements, but also bimolecular rate constants of quenching; the dynamic quenching of HSA phosphorescence by BPA is higher at pH 7.0 than at pH 9.0. The results obtained illustrate that time-resolved fluorescence and phosphorescence spectroscopy are appropriate tools to study HSA-ligand interactions at two complementary timescales.

References

(1) Varshney, A.; Sen, P.; Ahmad, E.; Rehan, M.; Subbarao, N.; Khan, R. H. *Chirality* **2010**, *22*, 77-87.

(2) Dockal, M.; Carter, D. C.; Rüker, F. *J. Biol. Chem*., **1999**, *274*, 29303-29310.

(3) Sułkowska A. *J. Molec. Struct.*, **2002**, *614*, 227-232.

(4) Martínez-Gómez, M. A.; Carril-Avilés, M. M.; Sagrado, S.; Villanueva-Camañas, R. M.; Medina-Hernández, M. J. *J. Chromatogr. A* **2007**, *1147*, 261-269.

(5) Martínez-Gómez, M. A.; Sagrado, S.; Villanueva-Camañas, R. M.; Medina-Hernández, M. J. *Electrophoresis* **2006**, *27*, 3410-3419.

(6) Yoo, M. J.; Schiel, J. E.; Hage, D. S. *J. Chromatogr. B* **2010**, *878*, 1707-1713.

(7) Chadborn, N.; Bryant, J.; Bain, A. J.; O'Shea, P. *Biophys. J*. **1999**, *76*, 2198-2207.

(8) Sudlow G.; Birkett, D. J.; Wade, D. N. *Clin. Experim. Pharmacol. Physiol*. **1975**, *2*, 129-140.

(9) Lakowicz, J. R. *Principles of fluorescence spectroscopy*, 3rd ed.; Springer: New York, 2006.

(10) Calhoun, C. B.; Vanderkooi, J. M.; Englander, S. W. *Biochemistry* **1983**, *22*, 1533-1539.

(11) Eftink, M. R.; Selvidge, L. A. *Biochemistry* **1982,** *21*, 117-125.

(12) Gonzalez-Jimenez, J.; Frutos, G.; Cayre, I.; Cortijo, M. *Biochimie* **1991**, *73*, 551-556.

(13) Saviotti, M. L.; Galley, W. C. *Proc. Nat. Acad. Sci. USA* **1974**, *71*, 4154-4158.

(14) Wei, Y.; Dong, C.; Liu, D.; Shuang, S.; Huie, C. W. *Biomacromolecules* **2007**, *8*, 761-764.

(15) Cioni, P.; Gabellieri, M.; Gonnelli, M.; Strambini, G. B. *Biophys. Chem*. **1994**, *52*, 25-34.

(16) Schlyer, B. D.; Schauerte, J. A.; Steel, D. G.; Gafni, A. *Biophys. J.* **1994**, *67*, 1192-1202.

(17) Telepchak, M. J.; Chaney, G.; August, T. F. *Forensic and clinical applications of solid phase extraction;* Humana Press Inc.: Totowa, 2004.

(18) Amiri, M.; Jankeje, K.; Albani, J. R. *J. Pharm. Biomed. Anal.* **2010**, *51*, 1097-1102.

(19) Otosu, T.; Nishimoto, E.; Yamashita, S. *J. Biochem*. **2010**, *147*, 191-200.

(20) Eftink, M. R.; Ghiron, C. A. *Anal. Biochem*. **1981**, *114*, 199-227.

Chapter 8

Interaction with human serum albumin:

Fluorescence and phosphorescence study for naproxen enantiomers

I. Lammers, V. Lhiaubet-Vallet, F. Ariese, M. A. Miranda, and C. Gooijer

Submitted for publication

Abstract

The interaction of the enantiomers of the non-steroidal anti-inflammatory drug naproxen (NPX) with human serum albumin (HSA) has been investigated using fluorescence and phosphorescence spectroscopy in the steady-state and time-resolved mode. The absorption, fluorescence excitation, and fluorescence emission spectra of (*S*)-NPX and (*R*)-NPX differ in shape in the presence of HSA, indicating that these enantiomers experience a different environment when bound. In solutions containing 0.2 M KI, complexation with HSA results in a strongly increased NPX fluorescence intensity and a decreased NPX phosphorescence intensity due to the inhibition of the collisional interaction with the heavy atom iodide. No significant difference was found between the binding constants derived from the fluorescence change: $(3.8\pm0.6)\times10^5$ M^{-1} for (*S*)-NPX and $(3.9\pm0.6)\times10^5$ M^{-1} for (*R*)-NPX. Furthermore, the addition of NPX quenches the phosphorescence of the single tryptophan in HSA (Trp-214) based on Dexter energy transfer. The short-range nature of this mechanism explains the upward curvature of the Stern-Volmer plot observed for HSA. At low concentrations NPX binds to HSA at a distance from Trp-214 and no quenching occurs, whereas at high NPX concentrations the phosphorescence intensity decreases due to dynamic quenching by NPX diffusing into site I from the bulk solution. The dynamic quenching observed in the Stern-Volmer plots based on the longest phosphorescence lifetime indicates an overall HSA binding constant of about 3×10^5 M^{-1} for both enantiomers.

8.1 Introduction

Human serum albumin (HSA) is the most abundant blood plasma protein. It plays an important role in the transport of a broad range of compounds, including many drugs.[1] The reversible interaction of drugs with HSA has a large influence on their pharmacological properties since only the unbound fraction in plasma is active; the maximum intensity of the therapeutic effect decreases for strongly bound drugs, while the gradual release of the bound fraction extends the duration of drug action.[2] Therefore, the potentially different binding of drug enantiomers to HSA can cause a difference in their biological properties.[3,4] Two main sites have been assigned for the binding of drugs to HSA.[5,6] Differentiation in the association of drug enantiomers is generally related to binding with Sudlow's site II, which has a narrower and less flexible cavity than Sudlow's site I.[7,8] The only tryptophan of HSA (Trp-214) near site I[1] is partially solvent-exposed.[9,10] The relatively long-wavelength absorption, high extinction coefficient, and high luminescence quantum yields of this amino acid have enabled the investigation of ligand binding using its intrinsic fluorescence[11-14] or phosphorescence[10,15] emission.

Fluorescence and phosphorescence can provide complementary information. An important difference is that excited singlet-state lifetimes of Trp in proteins are of the order of nanoseconds,[16,17] whereas the excited triplet-state lifetimes can be found in the range of milliseconds to seconds after deoxygenation.[18,19] This makes phosphorescence much more sensitive for dynamic quenching processes because quenchers have more time for diffusion. Also the main mechanism of energy transfer, which can cause quenching of Trp luminescence upon ligand binding, is different. Förster resonance energy transfer[20] (FRET) in fluorescence is based on Coulombic interactions and can occur over relatively long distances, in favorable cases up to 100 Å. In triplet-triplet energy transfer, two forbidden transitions are involved and Dexter energy transfer[21] based on electron exchange dominates. This interaction requires orbital overlap of the donor and acceptor and only occurs over short distances up to 10 Å. Therefore, a drug molecule needs to closely approach or collide with the Trp moiety in HSA for effective quenching of protein phosphorescence.

Naproxen ((*S*)- or (*R*)-NPX; Figure 8.1) is a 2-arylpropionic acid derivative belonging to the group of non-steroidal anti-inflammatory drugs.[22] In contrast to the racemic administration of most therapeutics in this group, the pharmaceutically active (*S*)-NPX is marketed enantiopure.[23] NPX is known to associate preferentially to site II of HSA, although site I is also populated to some extent.[24]

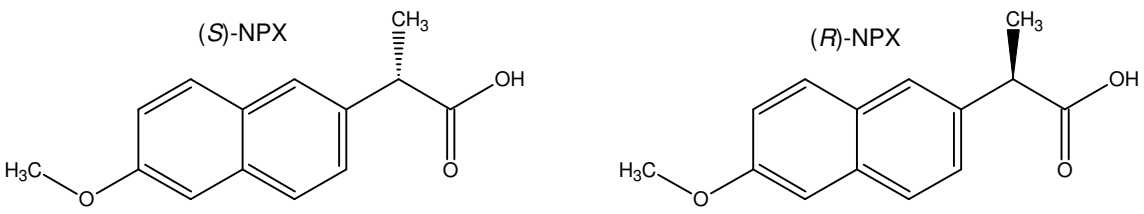

Figure 8.1: Molecular structures of the naproxen enantiomers.

Recently, several spectroscopic studies have been performed to investigate the binding of (*S*)-NPX and (*R*)-NPX to HSA. Upon complex formation, the Trp-214 fluorescence of HSA is mainly statically quenched.[24] The observation of an increased NPX emission after complexation with HSA has been interpreted as a minor contribution from energy transfer due to a relatively large distance between Trp-214 and NPX.[25] Furthermore, laser flash photolysis experiments indicated a difference in distribution of (*S*)-NPX and (*R*)-NPX over the two HSA binding sites, based on triplet excited state lifetimes of these ligands in aerated solutions.[24]

Direct room-temperature phosphorescence (RTP) in the liquid state has been used for the determination of (*S*)-NPX in pharmaceutical preparations and biological samples. In general, a heavy atom was used to enhance the phosphorescence signal and sample solutions were deoxygenated by adding sodium sulfite as an oxygen scavenger to prevent phosphorescence quenching by dissolved oxygen. A clear phosphorescence signal can be obtained for (*S*)-NPX under these conditions,[26] which is further enhanced in the presence of micelles[27-32] or cyclodextrins.[27,28] Recently, RTP has been used for the chiral discrimination between (*S*)-NPX and (*R*)-NPX in the presence of β-CD and 1,2-dibromoethane.[33] However, to the best of our knowledge, RTP has not been used before to study the interaction of (*S*)-NPX and (*R*)-NPX with HSA.

Although HSA contains only a single tryptophan moiety, the interpretation of HSA luminescence quenching for studying the interaction with ligands is not straightforward. Not only the presence of distinct binding sites complicates the analysis,[24] but also the existence of different HSA conformations in solution.[9,17] In the present chapter, the stereoselective binding of (*S*)-NPX en (*R*)-NPX to HSA is investigated using a combination of fluorescence and phosphorescence techniques. Note that the long-wavelength absorption of NPX enables the selective excitation of this ligand and that also the luminescence of HSA can be readily distinguished from that of NPX. This enables the comparison of quantitative binding information from the fluorescence of the ligand NPX and the time-resolved phosphorescence of HSA.

8.2 Experimental section

8.2.1 Chemicals

Fatty acid free albumin from human serum (≥ 96%), (*S*)-(+)-naproxen, (*R*)-(-)-naproxen, potassium iodide, sodium sulfite, and methanol were purchased from Sigma-Aldrich (St. Louis, MO, USA). Potassium monohydrogen phosphate and potassium dihydrogen phosphate were obtained from J.T. Baker B.V. (Deventer, the Netherlands). All chemicals were used as received. Water was purified with a Milli-Q system from Millipore (Bedfort, MA, USA).

8.2.2 Instrumentation

A Cary 50 spectrometer (Varian, Melbourne, Australia) was used for the absorption measurements with a spectral resolution of 1.5 nm using 10-mm square quartz cuvettes. Fluorescence and phosphorescence measurements were recorded with a Cary Eclipse luminescence spectrometer (Varian, Melbourne, Australia). The temperature of the samples was kept at 20°C using a single-cell Peltier cooler. The excitation and emission spectral band widths were set to 5 or 1.5 nm for fluorescence and to 10 nm for phosphorescence measurements. Excitation was performed at 290 nm (HSA, L-Trp and NPX) or 331 nm (NPX). The phosphorescence emission spectra were recorded with a delay time of 0.1 ms and a total gate time of 5 ms. The intensities were corrected for the signal loss during the delay time by multiplication with a correction factor depending on the lifetimes. Phosphorescence decay curves from 0.05 to 20 ms were obtained with an excitation wavelength of 290 nm (HSA and NPX) or 331 nm (NPX), an emission wavelength of 420 nm (HSA) or 545 nm (NPX), a gate width of 50 μs, and 1000 cycles. Using OriginPro 8.0 these decay curves were fitted with a bi-exponential decay function. Gnuplot 4.2.4 was used to fit the fluorescence curves of NPX.

Time-correlated single-photon counting (TCSPC) was used to record fluorescence decays. The excitation source was a Ti:Sapph laser (Coherent, Mira 900, Santa Clara, CA, USA) with a pulse width of 3 ps. The output of the laser was frequency tripled to get an excitation wavelength of 290 nm. A pulse picker was applied to reduce the laser repetition rate to 4 MHz. A multichannel-plate photomultiplier (Hamamatsu, R3809U-50, Japan) detected the fluorescence emission after being dispersed by a monochromator (TVC JarrellAsh Monospec 18, Grand Junction, CO, USA). Decays were recorded at emission wavelengths between 330 and 400 nm in 10 nm steps. An SPC-630 module (Becker & Hickl GmbH, Berlin, Germany) collected the data with a time resolution of 15 ps. A reflection of the laser pulse focused on a photodiode provided the synchronization signal for TCSPC. The instrument response function was determined by collecting scattered light from a suspension of silica particles and used for deconvolution of the recorded decays. The program Fluofit 4.2.9 was used to fit the data with a mono-exponential decay (NPX), a tri-exponential decay (HSA), or a tetra-exponential decay (HSA and NPX). For the tetra-exponential fit, the starting values for the HSA lifetimes were derived from the corresponding tri-exponential fit of HSA.

8.2.3 Procedure

Ligand stock solutions of 5 mM (*S*)-NPX and (*R*)-NPX were made in methanol. Absorption measurements were used to verify that the enantiomer concentrations were equal. Samples with different concentrations of the NPX enantiomers were obtained by evaporating the methanol from various volumes of the stock solutions before adding a solution of 10 μM HSA, 0.2 M KI, and 0.01 M phosphate buffer (pH 7.4). Deoxygenation was performed chemically with 0.2 mM Na_2SO_3 added to the sample directly before closing the cuvettes with

a stopper. The stock solutions of 0.2 M Na_2SO_3 were freshly prepared each day in deionized water. The absorbance of the NPX enantiomers at half cuvette length did not exceed 0.03.

8.3 Results and discussion

The large difference in the absorption and luminescence wavelengths of NPX and HSA as shown in Figure 8.2 makes it possible to study the effects of drug-protein interaction on their fluorescence and phosphorescence properties independently. First the influence on the NPX luminescence is addressed using selective excitation followed by the discussion of the influence on the HSA luminescence through selective emission detection. Note that most experiments were performed in the presence of 0.2 M KI, resulting in a reasonable fluorescence and a strong phosphorescence emission of Trp-214.[15]

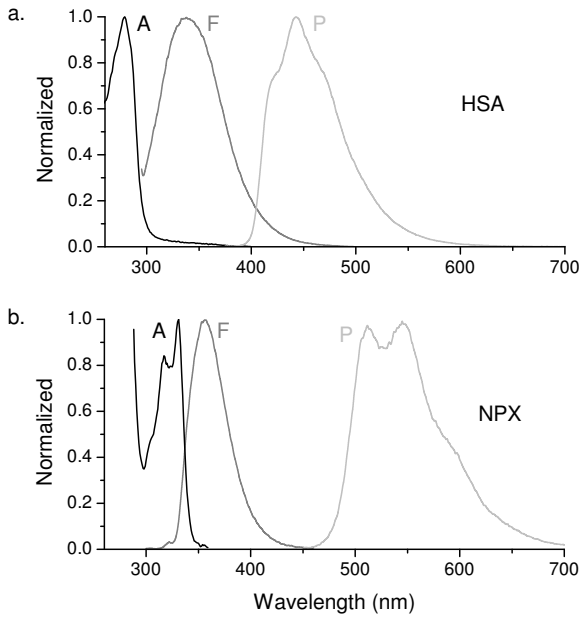

Figure 8.2: Normalized absorption (A), fluorescence emission (F) and phosphorescence emission (P) spectra of (a) 10 µM HSA and (b) 50 µM (*S*)-NPX. All samples were made in 0.01 M phosphate buffer (pH 7.4). Absorption spectra were obtained in the absence of KI without deoxygenation. The fluorescence and phosphorescence spectra were recorded after addition of 0.2 M KI and deoxygenation using 2 mM Na_2SO_3.

8.3.1 NPX luminescence

Since the absorption spectrum of NPX extends much further to the red than that of HSA, this drug can be excited close to its absorbance maximum at 331 nm without affecting the energy state of the protein (Figure 8.2). The fluorescence excitation and emission spectra of the two NPX enantiomers are identical to each other in water and in octane (Figure 8.3a and b) as expected in an achiral environment. However, the spectra show a more pronounced vibrational pattern in octane than in water. The vibrational pattern in the presence of HSA (Figure 8.3c) might indicate that the two NPX enantiomers experience a more apolar environment with respect to water after binding to HSA. Interestingly, the fluorescence

excitation and emission spectra of (*S*)-NPX and (*R*)-NPX are no longer identical upon complexation with HSA, but differ significantly. The same is observed in the absorption spectra above 300 nm (data not shown). These differences cannot be ascribed to the presence of KI in the HSA samples; in absence of this heavy atom salt identical spectral shapes are obtained (data not shown). Therefore, the spectral differences indicate that (*S*)-NPX and (*R*)-NPX are bound differently to HSA and experience a different local environment.

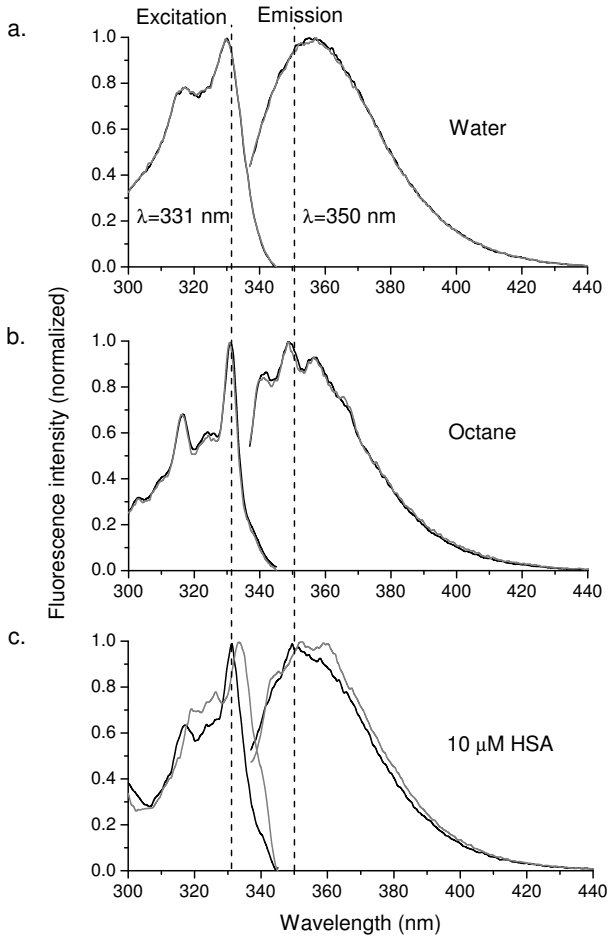

Figure 8.3: Normalized fluorescence excitation and emission spectra of 10 μM (*S*)-NPX (black trace) or (*R*)-NPX (gray trace) in (a) deionized water, (b) octane, and (c) 10 μM HSA in 0.01 M phosphate buffer (pH 7.4) with 0.2 M KI. Excitation spectra were recorded with an emission wavelength of 350 nm, and emission spectra were recorded with an excitation wavelength of 331 nm.

Figure 8.4a shows the fluorescence intensities of increasing concentrations of (*S*)-NPX and (*R*)-NPX in the presence and absence of 10 μM HSA. As expected, the NPX intensities in absence of HSA increase linearly with the concentration. (Note that no major inner filter effects due to the addition of NPX are observed under the applied conditions.) In the presence of 10 μM HSA, however, the initial slopes of the fluorescence increase of the NPX enantiomers are much higher. This indicates that the fluorescence intensity of NPX increases considerably upon complexation with HSA. The fluorescence increase declines at NPX concentrations above 10 μM (corresponding to a 1:1 complexation with a high-affinity site of

HSA) and eventually the slope becomes similar to the fluorescence increase in absence of HSA. Note that the small difference between the intensities of (*S*)-NPX and (*R*)-NPX in the presence of HSA does not necessarily correspond to different binding constants of these enantiomers with HSA, but can be related to the difference in the shape of their absorption and fluorescence emission spectra after binding (Figure 8.3c).

Although the shapes of the fluorescence emission spectra of (*S*)-NPX and (*R*)-NPX change upon binding to HSA, the phosphorescence emission spectral shapes are fully identical (data not shown). The phosphorescence intensities of the NPX enantiomers as a function of concentration are shown in Figure 8.4b. Note that the relation between the phosphorescence intensity and the NPX concentration in presence of HSA is not linear either. The effect of the complexation on the phosphorescence is opposite to that in fluorescence; the slope of the phosphorescence curve is smaller at lower NPX concentrations and increases at higher NPX concentrations. Eventually, it does not become similar to the slope in absence of HSA. Possibly, HSA partially quenches the phosphorescence of NPX free in solution or affects the intersystem crossing caused by collisions with iodide through increased viscosity. Similar to the fluorescence experiments in Figure 8.4a, the difference in intensity between (*S*)-NPX and (*R*)-NPX can be attributed to the difference in their absorption at 331 nm after complexation with HSA.

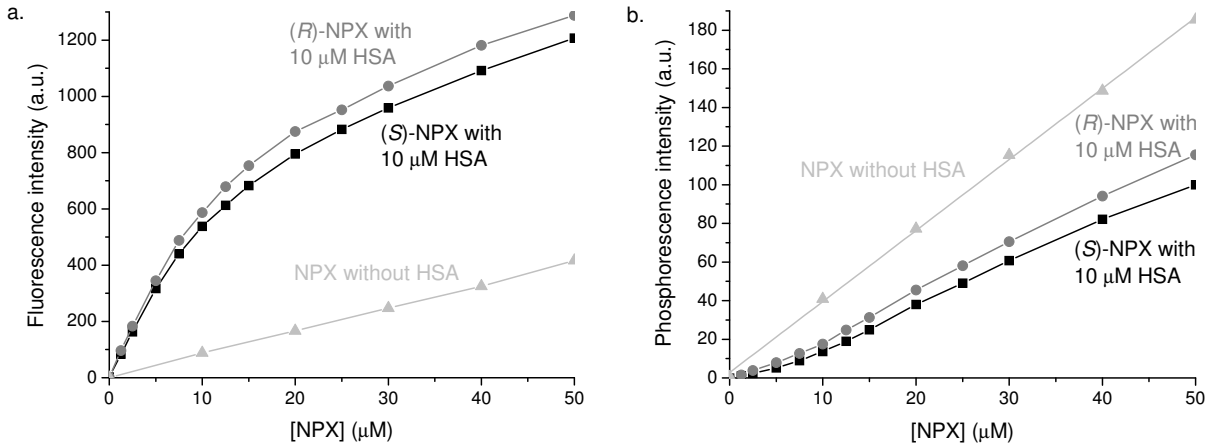

Figure 8.4: (a) Fluorescence intensity and (b) phosphorescence intensity of (*S*)-NPX in the presence of 10 μM HSA (■), (*R*)-NPX in the presence of 10 μM HSA (●), and (*S*)-NPX in absence of HSA (▲). All samples were made in 0.01 M phosphate buffer (pH 7.4) with 0.2 M KI for enhanced intersystem crossing and 2 mM Na_2SO_3 for deoxygenation. Xenon-lamp excitation was performed at 331 nm, and emission was monitored at 350 nm for fluorescence and 545 nm for phosphorescence.

The difference between the phosphorescence intensity of bound and unbound NPX is too small to accurately derive HSA binding constants from Figure 8.4b. However, the binding constants can be readily calculated from the large change in NPX fluorescence intensity upon association with HSA in the presence 0.2 M KI (Figure 8.4a). These calculations are based on

the assumption that the intensity change in fluorescence results from binding to one high affinity site,[34] *i.e.*, obeying the 1:1 interaction

$$P + L \leftrightarrows PL$$

where *P* is the protein HSA and *L* is the ligand NPX. The binding constant can be expressed as a function of the total concentrations (bound + unbound) protein and ligand

$$K = \frac{PL}{P \times L} = \frac{PL}{(P_t - PL)(L_t - PL)} \qquad \textbf{Eq. 8.1}$$

where *K* is the binding constant, *PL* is concentration of the HSA-NPX complex, *P* is the unbound HSA concentration, P_t is the total HSA concentration (10×10^{-6} M), *L* is the unbound NPX concentration, and L_t is the total NPX concentration. Equation 8.2 describes *PL* as a function of the increasing L_t concentrations.

$$PL(L_t) = \frac{1}{2} \times \left(L_t + P_t + K^{-1} - \sqrt{(L_t + P_t + K^{-1})^2 - 4L_tP_t} \right) \qquad \textbf{Eq. 8.2}$$

The binding constants can be derived from Figure 8.4a by combining this expression for the concentration of the NPX-HSA complex with

$$F(L_t) = S_L \times \left(L_t - PL(L_t) \right) + S_{PL} \times PL(L_t) \qquad \textbf{Eq. 8.3}$$

where *F* is the measured fluorescence intensity, slope S_L is proportional to the fluorescence of NPX free in solution, and slope S_{PL} is proportional to the fluorescence of bound NPX. The results of the fitting procedure are assembled in Table 8.1. The fluorescence slope of ligand free in solution is equal for the two NPX enantiomers as expected in an achiral environment. The differences in the fluorescence slopes of bound (*S*)-NPX and (*R*)-NPX correspond with the shifts in their excitation and emission spectra upon binding to HSA. Note that the NPX fluorescence intensity increases strongly, about a factor of 8, upon association with HSA. This result will be further discussed below. Although in view of the spectral shapes the binding of NPX to HSA is distinctly enantioselective, no significant difference was found between the binding constants of (*S*)-NPX and (*R*)-NPX of $(3.8\pm0.6)\times10^5$ and $(3.9\pm0.6)\times10^5$ M^{-1}, respectively. Binding constants of the same order of magnitude have been reported in the literature.[24,34]

Table 8.1: Fluorescence intensity slopes of NPX free in solution and of NPX bound to HSA, and the binding constants of the NPX enantiomers to HSA as derived from Figure 8.4a. Excitation was performed at 331 nm and emission was detected at 350 nm.

Enantiomer	S_L **(a.u.)**	S_{PL}**(a.u.)**	K **(M^{-1})**
(*S*)-NPX	$(1.08\pm0.06)\times10^7$	$(8.2\pm0.3)\times10^7$	$(3.8\pm0.6)\times10^5$
(*R*)-NPX	$(1.08\pm0.07)\times10^7$	$(9.1\pm0.3)\times10^7$	$(3.9\pm0.6)\times10^5$

The experiments for Figure 8.4 were performed in the presence of 0.2 M KI for optimal comparison of the fluorescence and the phosphorescence results. Similar fluorescence trends are observed in the absence of KI, although the relative difference in the intensity of bound and unbound NPX is much lower (data not shown). This indicates that the fluorescence intensity increase upon binding is largely caused by a decreased accessibility of complexed NPX for iodide. This same effect is probably involved in the decrease in phosphorescence emission of NPX upon complexation (Figure 8.4b). Energy transfer from Trp-214 to NPX does not play a role in the strong fluorescence intensity increase upon binding, since NPX is selectively excited at a wavelength of 331 nm where HSA does not absorb. Time-resolved fluorescence experiments using laser excitation at 290 nm were performed to further investigate changes in the NPX fluorescence quantum yield upon complexation with HSA in absence or presence of KI in aerated solutions. The lifetime data are assembled in Table 8.2.

Table 8.2: Fluorescence lifetimes of 10 µM HSA and/or 10 µM NPX in absence or presence of 0.2 M KI resulting from time correlated single photon counting. Laser excitation was performed at 290 nm and the emission was measured between 330 and 400 nm in 10 nm steps followed by a global fitting procedure. Duplicate measurements indicated standard deviations of 0.5 ns.

Sample	**HSA**			**NPX**
	τ_1 **(ns)**	τ_2 **(ns)**	τ_3 **(ns)**	τ **(ns)**
NPX	-	-	-	9.7
NPX + KI	-	-	-	1.3
HSA	7.2	2.7	0.3	-
HSA + KI	5.0	1.6	0.3	-
HSA + (*S*)-NPX	7.7	2.6	0.3	12.3
HSA + (*R*)-NPX	7.5	2.7	0.3	11.5
HSA + (*S*)-NPX + KI	5.5	1.6	0.4	10.4
HSA + (*R*)-NPX + KI	4.7	1.6	0.4	10.8

Table 8.2 indicates that without KI the fluorescence lifetime of the NPX enantiomers increases only 20% upon complexation to HSA from 9.7 ns to about 12 ns, although other authors did not observe such a lifetime increase under similar conditions.[24,35] In presence of KI, however, the increase is much larger: from 1.3 ns to about 10.6 ns. This factor of 8 difference between the fluorescence lifetime of NPX free in solution and NPX complexed to HSA corresponds well with the difference in slopes observed in Figure 8.4a and Table 8.1. The reason for the different effects in the absence and presence of KI becomes clear from Table 8.2: The fluorescence of free NPX is efficiently quenched by KI resulting in a lifetime change from 9.7 to 1.3 ns (about 87%), while the quenching of the NPX fluorescence in the HSA complex is much less pronounced from average 12 ns to average 10.6 ns (about 11%). Apparently, after complexation NPX is effectively protected against collisional interaction with KI. This is in line with the preferential positioning of NPX in the rather tight site II.[35]

8.3.2 HSA luminescence

Apart from the emission of the ligand, one can also study the luminescence of the protein in order to obtain information on binding processes. The HSA fluorescence quenching by NPX has recently been published by González-Béjar *et al.*[24] and is attributed to static quenching. Note that static quenching is based on the formation of a non-fluorescent ground-state complex between HSA and NPX and can be represented by Equation 8.4[16]

$$\frac{I_0}{I} = 1 + K[Q] \qquad \textbf{Eq. 8.4}$$

where I_0 and I are the luminescence intensities in absence and presence of quencher, respectively, K is the binding constant for the formation of the non-luminescent complex, and $[Q]$ is the quencher concentration. The luminescence lifetime should not change in case of static quenching, which is fully in line with our data in Table 8.2; the three HSA fluorescence lifetimes observed do not decrease in the presence of NPX.

In contrast to the HSA fluorescence quenching study published,[24] the focus of this section is on the phosphorescence emission of HSA for studying the complexation of the NPX enantiomers. At the excitation wavelength of 290 nm, mainly Trp-214 of HSA and NPX are excited and the absorption of other amino acid residues is minor.[16] The NPX phosphorescence is shifted to the red with respect to the HSA phosphorescence, which enables the isolation of the latter by selecting an emission wavelength of 420 nm.

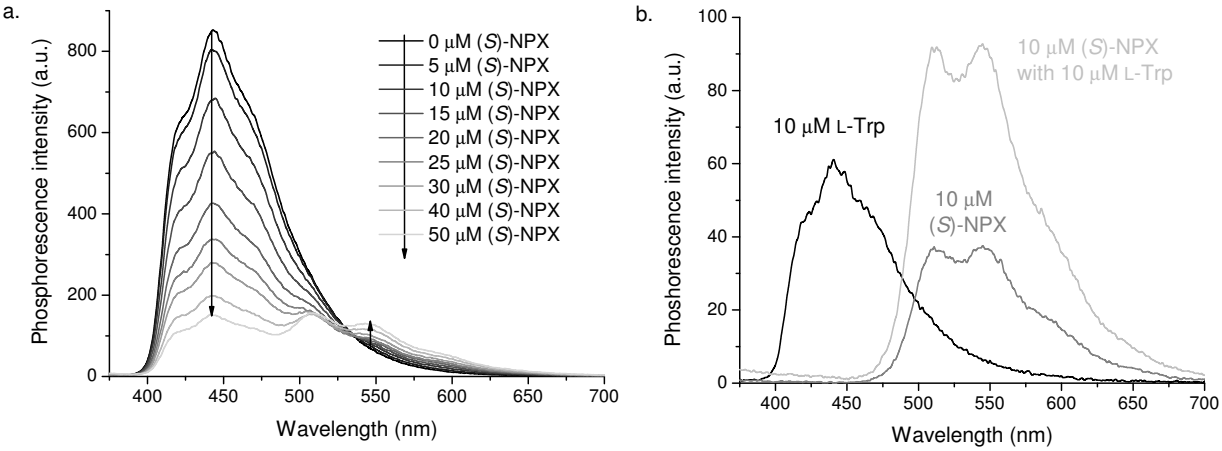

Figure 8.5: Phosphorescence emission spectra of (a) 10 μM HSA with increasing concentrations of (*S*)-NPX and (b) 10 μM L-Trp and/or 10 μM (*S*)-NPX. All samples were made in 0.01 M phosphate buffer (pH 7.4) with 0.2 M KI to enhance the intersystem crossing and 2 mM Na_2SO_3 for deoxygenation. Excitation was performed at 290 nm with a pulsed xenon lamp.

The addition of increasing (*S*)-NPX concentrations to 10 μM HSA in the presence of 0.2 M KI causes a gradual decrease in the HSA phosphorescence intensity as shown in Figure 8.5a. In order to study the quenching mechanism, the phosphorescence of the free amino acid

L-Trp was recorded in the absence and presence of (*S*)-NPX for comparison. The spectra in Figure 8.5b indicate an efficient triplet-triplet energy transfer from L-Trp to (*S*)-NPX; the L-Trp phosphorescence is completely quenched by 10 μM (*S*)-NPX, while the phosphorescence signal of the latter is about 2.5-fold enhanced. The quenching of HSA induced by 10 μM (*S*)-NPX is much lower (Figure 8.5a); the signal reduction of HSA phosphorescence is only 20%, while the phosphorescence signal of (*S*)-NPX remains relatively low after complexation with HSA. Note that the increase in the (*S*)-NPX signal as a result of the minor energy transfer from HSA will be counterbalanced by the decrease in (*S*)-NPX phosphorescence quantum yield upon binding to HSA as was concluded from Figure 8.4b. The results obtained with (*R*)-NPX were similar (data not shown).

The P_0/P Stern-Volmer plots for quenching of the HSA phosphorescence intensity by the two NPX enantiomers recorded at 420 nm are shown in Figure 8.6a. They differ strongly from the F_0/F Stern-Volmer plots based on the fluorescence intensity (data not shown), which indicate that HSA fluorescence quenching starts immediately at low concentrations.[24] In contrast, the phosphorescence quenching is minor at low NPX concentrations and increases with increasing NPX concentrations.

Phosphorescence decay curves were recorded to discriminate between dynamic and static quenching. In contrast to static quenching, which is based on complex formation in the ground state, in dynamic or collisional quenching the quencher Q diffuses towards the fluorophore or phosphorophore during the lifetime of the excited state. In that case the intensity decrease is given by[16]

$$\frac{I_0}{I} = \frac{\tau_0}{\tau} = 1 + k_q \tau_0 [Q] \qquad \textbf{Eq. 8.5}$$

where τ_0 and τ are the luminescence lifetime in absence and presence of quencher, respectively, and k_q is the bimolecular quenching constant. Note that in this dynamic quenching the lifetime is reduced as well. The HSA phosphorescence decay curves were fitted with a bi-exponential decay; in absence of NPX lifetimes of 2.23±0.02 and 0.33±0.07 ms (n = 5) were found with amplitudes of 100±2 and 12.0±0.8 (n = 5), respectively. Such multi-component phosphorescence decays for proteins with a single Trp indicate the presence of various protein conformations that are stable on the phosphorescence timescale.[9,36,37] Figure 8.6b shows the Stern-Volmer plots based on the longest lifetime and its amplitude, because this HSA conformer contributes most to the total phosphorescence intensity.

The A_0/A Stern-Volmer plot based on the phosphorescence amplitude (Figure 8.6b) shows a large similarity to the F_0/F Stern-Volmer plot (data not shown) in the presence of 0.2 M KI. The relatively flat A_0/A Stern-Volmer plot indicates that the static component of the HSA phosphorescence quenching is minor. In comparison with the recent publication of González-Béjar *et al.*[24], the slope of the Stern-Volmer plot based on steady-state HSA

fluorescence is smaller in presence than in absence of 0.2 M KI (data not shown). The Stern-Volmer plot based on the phosphorescence lifetime (τ_0/τ in Figure 8.6b) indicates that the main quenching mechanism of the HSA phosphorescence is of a dynamic nature.

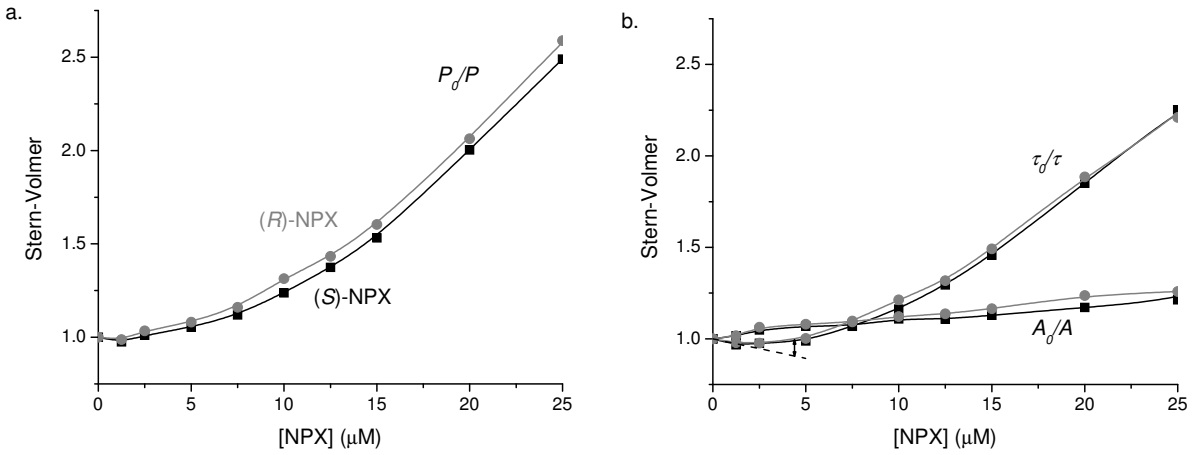

Figure 8.6: Stern-Volmer plots of the HSA phosphorescence quenching by (*S*)-NPX (■) or (*R*)-NPX (●) based on (a) the intensity P_0/P and (b) the longest lifetime τ_0/τ with corresponding amplitude A_0/A. All samples contained 10 μM HSA in 0.01 M phosphate buffer (pH 7.4) with 0.2 M KI for enhanced intersystem crossing and 2 mM Na_2SO_3 for deoxygenation. Xenon-lamp excitation was performed at 290 nm and emission was monitored at 420 nm, which is selective for HSA phosphorescence.

Unexpectedly, the HSA lifetime first slightly increases at low NPX concentrations, before it starts showing a clear dynamic quenching by NPX. This effect was also observed for other well-known and strong site II binders, including (*RS*)-ibuprofen, (*S*)-flurbiprofen, and octanoic acid (data not shown). The lifetime increase might be caused by a change in the protein environment around Trp-214 or an alteration in the accessibility to the heavy atom as a result of ligand binding to site II.[15]

The large deviation from linearity of the τ_0/τ Stern-Volmer plot is related to the Dexter energy transfer quenching mechanism, which requires a collisional interaction between NPX and Trp-214 in HSA. At low concentrations, NPX will be almost completely bound to HSA in site II and therefore cannot collide with Trp-214. At higher concentrations, the amount of NPX free in solution increases resulting in diffusion into site I and stronger dynamic quenching until it reaches a quenching constant of $(3.3\pm0.1)\times10^7$ M^{-1} s^{-1} (calculated with τ_0 = 2.23 ms) for both (*S*)-NPX and (*R*)-NPX. Note that this quenching constant is two orders of magnitude lower than the diffusion-controlled rate constant, which indicates that Trp-214 is protected against quenching inside the protein matrix.

In principle, the binding constant of HSA and NPX can be inferred from the phosphorescence τ_0/τ Stern-Volmer plot in Figure 8.6b. Since only NPX diffusing from the bulk solution into site I quenches the HSA phosphorescence, it reveals the concentration of NPX free in solution for each total NPX concentration added to the sample. Unfortunately, this is complicated by the fact that τ_0 is not constant but increases a little upon complexation

of NPX with HSA in site II. A rough estimation of the binding constant can be obtained by extrapolating this τ_0 increase linearly at low NPX concentrations (see dashed line in Figure 8.6b). For example, the 10% dynamic quenching point with respect to the extrapolated τ_0 is found at a total added NPX concentration of 4.4 µM NPX. Based on the slope ($k_q \cdot \tau_0$) of the linear part of the τ_0/τ Stern-Volmer plot at high NPX concentrations, the concentration of NPX free in solution at the 10% dynamic quenching point is 1.4 µM. Based on these values and a 1:1 complex stoichiometry, a binding constant of 3×10^5 M^{-1} is found, which is quite close to that derived from the NPX fluorescence. Note that the phosphorescence Stern-Volmer plots in Figure 8.6 do not reveal a significant difference between (*S*)-NPX and (*R*)-NPX.

8.4 Conclusions

Fluorescence and phosphorescence in the steady-state and time-resolved mode provide detailed information about the binding of NPX enantiomers to HSA. The absorption, fluorescence excitation, and fluorescence emission spectra of (*S*)-NPX and (*R*)-NPX have different shapes in the presence of HSA, indicating a stereoselective interaction. Whereas the fluorescence of NPX in solution is very efficiently quenched by iodide, the collisional interactions with this heavy atom are inhibited for NPX complexed with HSA. The intensity increase of the NPX fluorescence upon binding to HSA in the presence of iodide allows the calculation of binding constants. Furthermore, the phosphorescence of Trp-214 in HSA is dynamically quenched by NPX due to Dexter energy transfer. Non-linear Stern-Volmer plots are obtained that are indicative of the binding constants. The distance between Trp-214 and NPX bound to HSA is too large for Dexter energy transfer to occur and only NPX that can diffuse from the bulk solution into site I can collide with Trp-214 and cause quenching. Although the interaction of NPX and HSA is stereoselective, no difference in binding constants was observed based on NPX fluorescence or HSA phosphorescence.

References

(1) Peters, T. *All about albumin: Biochemistry, genetics, and medical applications;* Academic Press: London, 1996.

(2) Vuignier, K.; Schappler, J.; Veuthey, J.L.; Carrupt, P.A.; Martel, S. *Anal. Bioanal. Chem.* **2010**, 398, 53-66.

(3) Chuang, V. T. G.; Otagiri, M. *Chirality* **2006**, *18*, 159-166.

(4) Landoni, M. F.; Soraci, A. *Curr. Drug Metab.* **2001**, *2*, 37-51.

(5) Sudlow, G.; Birkett, D. J.; Wade, D. N. *Mol. Pharmacol.* **1975**, *11*, 824-832.

(6) Sudlow, G.; Birkett, D. J.; Wade, D. N. *Mol. Pharmacol.* **1976**, *12*, 1052-1061.

(7) Ascenzi, P.; Fasano, M. *Biophys. Chem.* **2010**, *148*, 16-22.

(8) Otagiri, M. *Drug Metab. Pharmacokinet.* **2005**, *20*, 309-323.

(9) Banks, D. D.; Kerwin, B. A. *Anal. Biochem.* **2004,** *324*, 106-114.

(10) Gabellieri, E.; Strambini, G. B.; Shcharbin, D.; Klajnert, B.; Bryszewska, M. *Biochim. Biophys. Acta* **2006**, *1764*, 1750-1756.

(11) Ge, F.; Chen, C.; Liu, D.; Han, B.; Xiong, X.; Zhao, S. *J. Lumin.* **2010**, *130*, 168-173.

(12) Matei, I.; Hillebrand, M. *J. Pharm. Biomed. Anal.* **2010**, *51*, 768-773.
(13) Naik, P. N.; Chimatadar, S. A.; Nandibewoor, S. T. *J. Photochem. Photobiol. B* **2010**, *100*, 147-159.
(14) Ding, F.; Liu, W.; Li, Y.; Zhang, L.; Sun, Y. *J. Lumin.* **2010**, *130*, 2013-2021.
(15) Wei, Y.; Dong, C.; Liu, D.; Shuang, S.; Huie, C. W. *Biomacromolecules* **2007**, *8*, 761-764.
(16) Lakowicz, J. R. *Principles of fluorescence spectroscopy*, 3rd ed.; Springer: New York, 2006.
(17) Amiri, M.; Jankeje, K.; Albani, J. R. *J. Pharm. Biomed. Anal.* **2010**, *51*, 1097-1102.
(18) Gonnelli, M.; Strambini, G. B. *Biochemistry* **1995**, *34*, 13847-13857.
(19) Vanderkooi, J. M.; Calhoun, D. B.; Englander, S. W. *Science* **1987**, *236*, 568-569.
(20) Förster, T. *Discuss. Faraday Soc.* **1959**, *27*, 7-17.
(21) Dexter, D. L. *J. Chem. Phys.* **1953**, *21*, 836-850.
(22) Todd, P. A.; Clissold, S. P. *Drugs* **1990**, *40*, 91-137.
(23) Kean, W. F.; Howard-Lock, H. E.; Lock, C. J. L. *Lancet* **1991**, *338*, 1565-1568.
(24) González-Béjar, M.; Alarcón, E.; Poblete, H.; Scaiano, J. C.; Pérez-Prieto, J. *Biomacromolecules* **2010**, *11*, 2255-2260.
(25) Vayá, I.; Pérez-Ruiz, R.; Lhiaubet-Vallet, V.; Jiménez, C. M.; Miranda, M. A. *Chem. Phys. Lett.* **2010**, *486*, 147-153.
(26) Segura-Carretero, A.; Cruces-Blanco, C.; Ramírez-García, M. I.; Cañabate-Díaz, B.; Fernández-Gutiérrez, A. *Talanta* **1999**, *50*, 401-407.
(27) Arancibia, J. A.; Escandar, G. M. *Analyst* **2001**, *126*, 917-922.
(28) Cline Love, L. J.; Grayeski, M. L.; Noroski, J.; Weinberger, R. *Anal. Chim. Acta* **1985**, *170*, 3-12.
(29) Panadero, S.; Gomez-Hens, A.; Pérez-Bendito, D. *Anal. Lett.* **1995**, *28*, 1405-1419.
(30) Pérez-Ruiz, T.; Martínez-Lozano, C.; Tomás, V.; Carpena, J. *J. Pharm. Biomed. Anal.* **1998**, *17*, 719-724.
(31) Rapado-Martínez, I.; Villanueva-Camañas, R. M.; García-Alvarez-Coque, M. C. *Analyst* **1994**, *119*, 1093-1097.
(32) Rekharskaya, E. M.; Polenova, T. V.; Borzenko, A. G. J. *Anal. Chem.* **2005**, *60*, 420-425.
(33) Wei, Y.; Wang, S.; Chao, J.; Wang, S.; Dong, C.; Shuang, S.; Chin Paau, M.; Choi, M. M. F. *J. Phys. Chem. C* **2011**, *115*, 4033-4040.
(34) Cheruvallath, V. K.; Riley, C. M.; Narayanan, S. R.; Lindenbaum, S.; Perrin, J. H. *Pharm. Res.* **1996**, *13*, 173-178.
(35) Thomas, M. P.; Nelson, G.; Patonay, G.; Warner, I. M. *Spectrochim. Acta* **1988**, *43B*, 651-660.
(36) Cioni, P.; Gabellieri, M.; Gonnelli, M.; Strambini, G. B. *Biophys. Chem.* **1994**, *52*, 25-34.
(37) Schlyer, B. D.; Schauerte, J. A.; Steel, D. G.; Gafni, A. *Biophys. J.* **1994**, *67*, 1192-1202.

Chapter 9

Interaction with human serum albumin:

Phosphorescence study for flurbiprofen enantiomers and their methyl esters

I. Lammers, V. Lhiaubet-Vallet, M. C. Jiménez, F. Ariese, M. A. Miranda, and C. Gooijer

Submitted for publication

Abstract

The interaction of the nonsteroidal anti-inflammatory drug flurbiprofen (FBP) with human serum albumin (HSA) hardly influences the fluorescence of the protein's single tryptophan. Therefore, in addition to fluorescence, heavy atom induced room-temperature phosphorescence is used to study the stereoselective binding of FBP enantiomers and their methyl esters to HSA. Maximal HSA phosphorescence intensities were obtained at a KI concentration of 0.2 M. The quenching of the tryptophan phosphorescence by FBP is mainly dynamic and based on Dexter energy transfer. The Stern-Volmer plots based on the phosphorescence lifetimes indicate that (R)-FBP causes a stronger tryptophan quenching than (*S*)-FBP. For the methyl esters of FBP the opposite is observed: (*S*)-FBPMe quenches more than (*R*)-FBPMe. The Stern-Volmer plots of (*R*)-FBP and (*R*)-FBPMe are similar although their high-affinity binding sites are known to be different. The methylation of (*S*)-FBP causes a large change in its effect on the HSA phosphorescence lifetime. Furthermore, the quenching constants of 3.0×10^{7} M^{-1} s^{-1} of the *R*-enantiomers and 2.5×10^{7} M^{-1} s^{-1} for the *S*-enantiomers are not influenced by the methylation and indicate a stereoselectivity in the accessibility of the HSA tryptophan to these drugs.

9.1 Introduction

The room-temperature phosphorescence (RTP) of tryptophan (Trp) residues in proteins has been shown to be a reliable probe for the local protein environment.[1-3] After deoxygenation, lifetimes of several seconds have been reported for Trp residues buried within the hydrophobic core of proteins,[4] whereas solvent-exposed Trp residues have triplet-state lifetimes in the (sub)millisecond range.[5,6] Also intermolecular interactions can influence the Trp phosphorescence; the effect of several external quenchers on protein phosphorescence has been investigated, ranging from small diatomic compounds[7,8] to larger molecules[9,10]. Depending on the quencher and macromolecule under study, the quenching process can be based on long-range through-space interactions or on collisional interactions. Such collisions require a degree of solvent-exposure of the Trp residue or a diffusion of the quencher through the protein matrix.[3,9,11]

RTP is in many aspects a complementary technique to fluorescence for studying the interaction of proteins and ligands. The spin-forbidden nature of the phosphorescence transition from the excited triplet state (T_1) to the singlet ground state (S_0) of Trp results in long intrinsic excited-state lifetimes. Compared with the fluorescence emission occurring at a nanosecond timescale, these long phosphorescence lifetimes enable the investigation of much slower dynamic processes.[1] The sensitivity of protein phosphorescence quenching is generally higher because there is more time for the interaction with quenchers.[3] Furthermore, the quenching mechanisms available for phosphorescence and fluorescence luminescence can be fundamentally different. The triplet-triplet energy transfer in phosphorescence quenching is based on the Dexter mechanism[12] of electron exchange, which requires a close contact between the donor and acceptor. For the singlet-singlet energy transfer in fluorescence, the Förster mechanism[13] usually dominates. This non-radiative process is based on Coulombic interactions that can occur over longer distances in space. Förster Resonance Energy Transfer (FRET) plays no role in phosphorescence since it is spin-forbidden.

Human serum albumin (HSA) is the most abundant circulatory protein and transports a broad range of endogenous and exogenous ligands. Two main binding sites have been identified in its interaction with drugs: site I and II.[14,15] The single Trp residue of HSA (Trp-214) is found near site I and has some degree of solvent accessibility.[10,16] Drug binding to HSA is often stereoselective, which can result in a difference in the metabolism, distribution, and elimination of enantiomers.[17] Therefore, it is very important to investigate the affinity of the separate enantiomers for HSA. Recently, phosphorescence lifetimes of bovine and human serum albumin (BSA and HSA) were used to discriminate between the enantiomers of various compounds.[18]

Flurbiprofen ((*S*)- or (*R*)-FBP; Figure 9.1) is a nonsteroidal anti-inflammatory drug of the 2-arylpropionic acid class with a chiral center at the carbon atom α to the carboxyl group.[19] Although FBP is currently administered as a racemic mixture, its enantiomers have distinct biological activities. The anti-inflammatory activity of FBP is predominantly

associated with the inhibition of cyclooxygenases by the *S*-enantiomer, which unfortunately also causes gastrointestinal toxicity upon prolonged use.[20] Flurbiprofen methyl esters ((*S*)- or (*R*)-FBPMe; Figure 9.1)[21,22] have been synthesized to improve the gastrointestinal tolerability by masking the carboxyl group to decrease accumulation in gastric mucosa.[20]

The interaction of the FBP enantiomers and their methyl esters with BSA and HSA has been investigated using laser flash photolysis.[23-25] The methylation potentially has a large influence on the interaction with transport proteins because the acidic FBP is negatively charged under physiological conditions, whereas FBPMe is neutral. Upon binding to BSA or HSA, the triplet-state lifetimes of FBP and FBPMe were characteristic for the enantiomers and the specific binding site involved. Based on the amplitudes belonging to the different lifetimes, Vaya and coworkers[23-25] reported that FBP has a preference for site II, whereas FBPMe has a higher affinity for site I.[17,24]

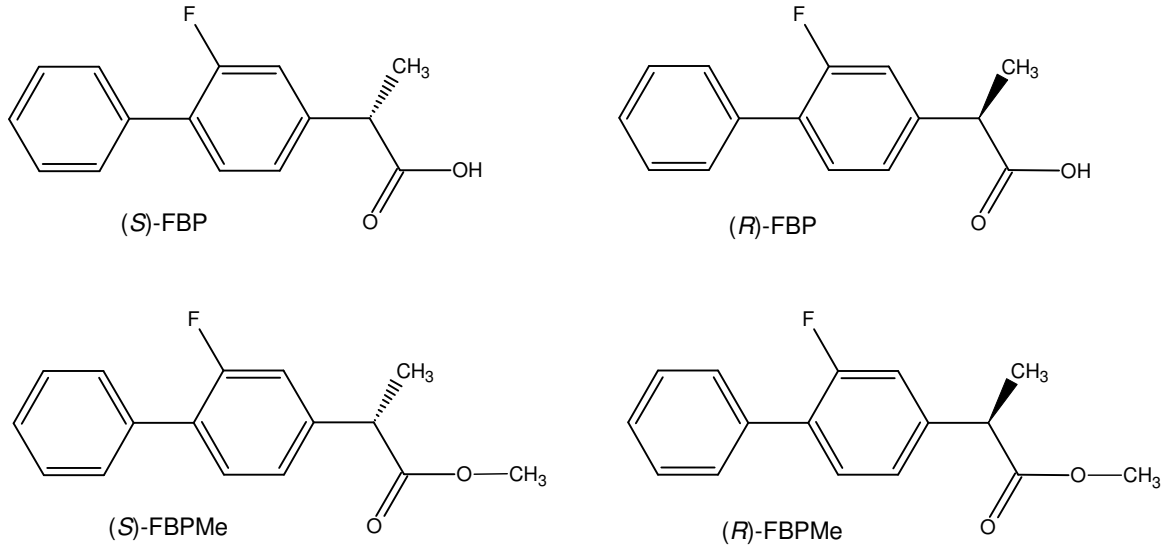

Figure 9.1: Molecular structures of the flurbiprofen enantiomers and their methyl esters.

These laser flash photolysis experiments[23-25] were performed without sample deoxygenation and focused on the spectroscopic properties of the FBP enantiomers and their methyl esters in the interaction with transport proteins. In the present chapter, however, we investigate how the stereoselective binding of these ligands affects the luminescence of HSA in absence of oxygen. After selecting an optimal heavy atom concentration to obtain maximum room-temperature phosphorescence intensity, the influence of the ligand binding on the steady-state fluorescence and the steady-state/time-resolved phosphorescence of Trp-214 in HSA is recorded to investigate static and dynamic ligand-protein binding processes.

9.2 Experimental section

9.2.1 Chemicals

Fatty acid free albumin from human serum (≥ 96%), (*S*)-flurbiprofen, (*R*)-flurbiprofen, potassium iodide, sodium sulfite, hydrochloric acid, and methanol were purchased from Sigma-Aldrich (St. Louis, MO, USA). The synthesis of the (*R*)- and (*S*)-flurbiprofen methyl esters has been described before.[25] TRIS was supplied by United State Biochemicals (Cleveland, OH, USA). All chemicals were used as received. Water was purified with a Milli-Q system from Millipore (Bedfort, MA, USA).

9.2.2 Instrumentation

A Cary 50 absorption spectrometer (Varian, Melbourne, Australia) was used for absorption measurements. A Cary Eclipse luminescence spectrometer (Varian, Melbourne, Australia) was used for recording fluorescence and phosphorescence. The temperature of the samples in square quartz cuvettes with 10 mm path length was kept at 20°C using a single-cell Peltier cooler. Excitation was performed at 290 nm. The fluorescence emission was measured at 340 nm and the phosphorescence emission at 443 nm (in absence of FBP or FBPMe) or 410 nm (in presence of FBP or FBPMe). Excitation and emission spectral band widths were set to 10 nm for phosphorescence and 5 nm for fluorescence measurements. The phosphorescence emission spectra were recorded with a delay time of 0.1 ms and a total gate time of 5 ms. The intensities were corrected for the signal loss during the delay time by multiplication with a correction factor depending on the lifetimes. Phosphorescence decay curves from 0.05 to 20 ms were obtained with a gate width of 50 µs and 1000 cycles. Using OriginPro 8.0, these decay curves were fitted with a bi-exponential decay function $P(t) = A_1 e^{-t/\tau_1} + A_2 e^{-t/\tau_2}$, where *P(t)* is the phosphorescence intensity as a function of time *t*, and A_1 and A_2 are the amplitudes belonging to the lifetimes τ_1 and τ_2.

9.2.3 Procedure

Ligand stock solutions of 5 mM (*S*)-FBP, (*R*)-FBP, (*S*)-FBPMe and (*R*)-FBPMe were made in methanol. Equal enantiomer concentrations were verified using absorption measurements. Samples were prepared by adding different volumes of the stock solutions to 5 or 10 µM HSA and 0.2 M KI in 0.01 M TRIS-HCl (pH 7.4). The presence of methanol did not influence the Stern-Volmer plots. Deoxygenation was performed chemically by adding Na_2SO_3 to the sample directly before closing the cuvettes with a stopper. Solutions of 0.2 M Na_2SO_3 were prepared fresh each day in deionized water. The final Na_2SO_3 concentration in all samples was 2 mM.

9.3 Results and discussion

9.3.1 Heavy atom

Iodide can be used as a heavy atom perturber to create a strong HSA phosphorescence.[18] Figure 9.2 shows the influence of the KI concentration on the HSA fluorescence and phosphorescence over a wide concentration range up to 2.0 M. Initially, the phosphorescence is enhanced with increasing KI concentrations (Figure 9.2b). The maximum phosphorescence intensity of HSA is obtained at a concentration of 0.2 M KI, which was selected as the optimum for further experiments. Note that its ionic strength is similar to that under physiological conditions. A further increase in KI concentrations causes a deterioration of the overall phosphorescence intensity. In order to explain this behavior we have to consider the influence of the heavy atom on the HSA luminescence in more detail.

The fluorescence quenching mechanism by iodide is based on the enhancement of intersystem crossing created by the heavy atom effect, which also causes the increase in phosphorescence emission at low KI concentrations. Figure 9.2a shows that the HSA fluorescence is not fully quenched by KI; even at the highest concentration of 2.0 M KI almost 40% of the original fluorescence persists. Furthermore, the fluorescence emission maximum shifts from 343 nm to 338 nm upon addition of 2.0 M KI (data not shown). Both observations could be consistent with the presence of different HSA conformations in solution, in which the accessibility of Trp-214 by iodide differs. Iodide is charged and does not readily penetrate the hydrophobic regions of a protein.[26,27] The conformations with a more accessible Trp-214 that have a red-shifted emission are more efficiently quenched, while the blue-shifted emission of conformations with a less accessible Trp-214 remains. This phenomenon might also be related with the observation that the HSA fluorescence decay has to be described by three lifetimes, despite the fact that it is a single-tryptophan protein.[27] Of course also the extreme ionic strengths at the high KI concentrations may play a role.

Also in phosphorescence more lifetimes play a role. A bi-exponential function was needed to fit the phosphorescence decay curves, resulting in two lifetimes (Figure 9.2c) with corresponding amplitudes (Figure 9.2d). Such multi-component phosphorescence decays for single Trp proteins indicate the presence of various protein conformations that are stable on the phosphorescence timescale.[28,29] Lifetimes of 2.7 and 0.4 ms were found at 0.2 M KI. The phosphorescence intensity is dominated by the long-lifetime component since its amplitude is about 6-fold higher as well. The phosphorescence intensity decrease at higher KI levels (Figure 9.2b) is accompanied by a similar shortening of the longest phosphorescence lifetime of HSA (Figure 9.2c). Apparently, the non-radiative pathway from T_1 to S_0 is enhanced more strongly than the radiative phosphorescence pathway. This outweighs the increase in triplet yield by intersystem crossing from S_1 to T_1, which levels off at the higher KI concentrations (Figure 9.2a). The phosphorescence emission spectra did not change in shape upon addition of KI (data not shown).

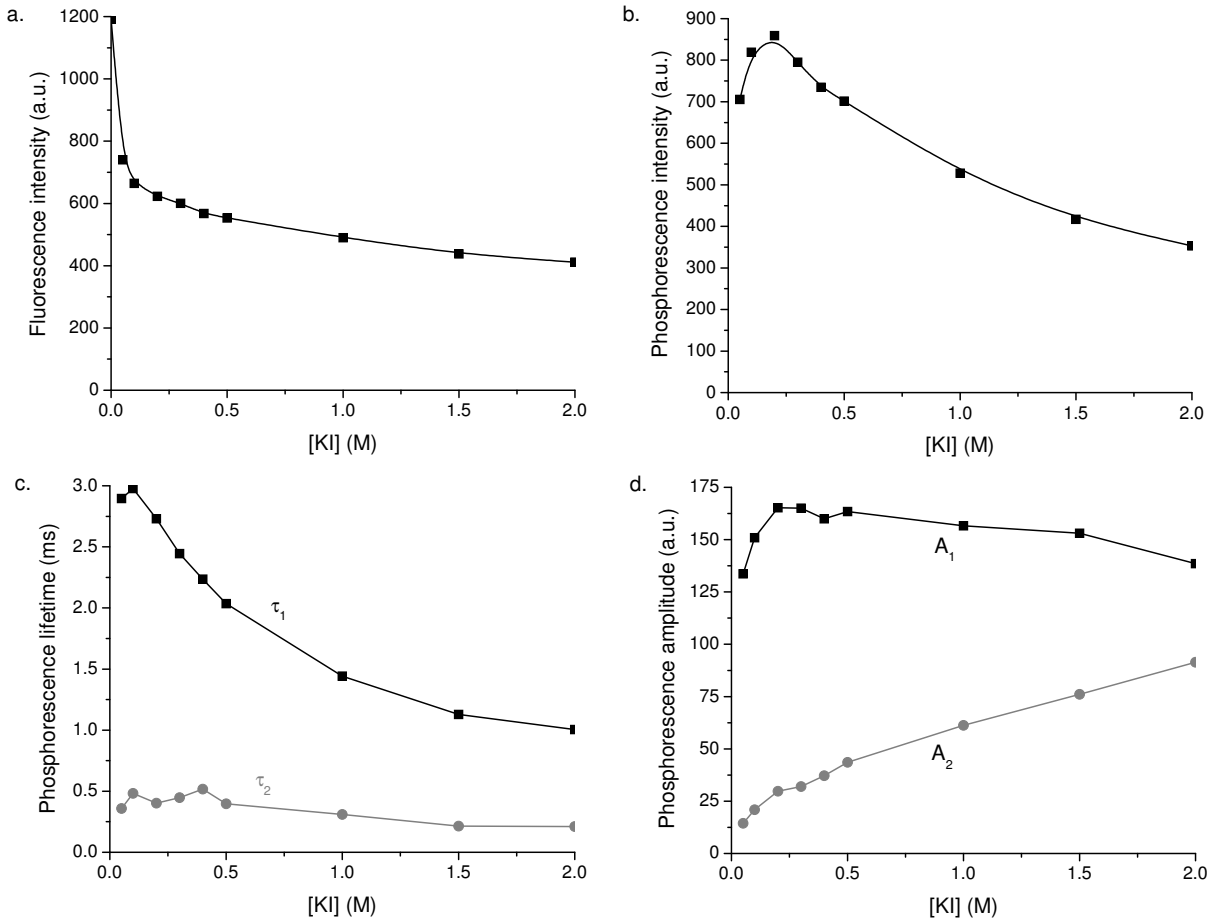

Figure 9.2: The influence of the KI concentration on the luminescence properties of 10 µM HSA: (a) fluorescence intensity, (b) phosphorescence intensity, and (c) phosphorescence lifetimes τ_1 (■) and τ_2 (●) with (d) corresponding amplitudes A_1 (■) and A_2 (●). Samples were buffered with 0.1 M TRIS-HCl (pH 7.4) and 2 mM Na_2SO_3 was used for deoxygenation. Xenon-lamp excitation was performed at 290 nm, fluorescence emission was measured at 340 nm and phosphorescence emission at 443 nm.

A disadvantage of iodide is its large absorption at shorter wavelengths, which may cause inner filter effects for the luminescence measurements. Only excitation wavelengths longer than 280 nm can be applied, which somewhat limits the experimental flexibility. Therefore, we also tested other heavy atoms with a lower absorption including bromide, thallium and cesium. Although bromide and thallium decreased the HSA fluorescence intensity, no phosphorescence enhancement was observed (data not shown).

9.3.2 Luminescence quenching

Increasing concentrations of the FBP enantiomers and their methyl esters were added to samples of 10 µM HSA with 0.2 M KI to investigate the quenching of the fluorescence and phosphorescence emission of HSA. All experiments were conducted with an excitation wavelength of 290 nm, where mainly the amino acid tryptophan of HSA is excited.[27] FBP has a very low extinction coefficient at this wavelength. See Figure 9.3 for the normalized absorption, fluorescence emission and phosphorescence emission spectra of HSA and (*S*)-FBP.

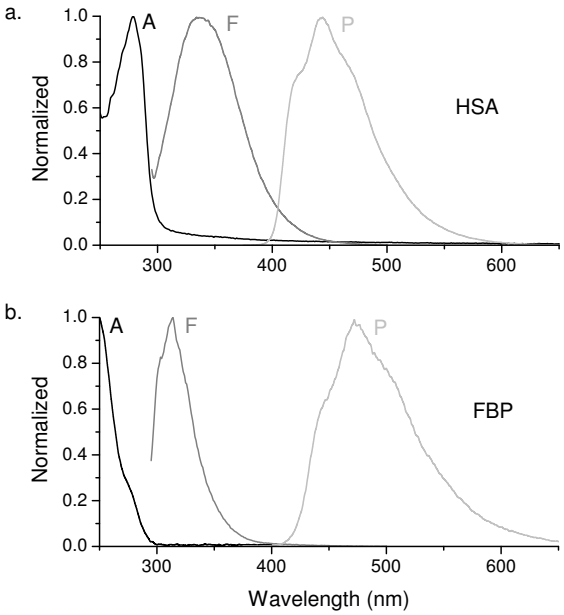

Figure 9.3: Normalized absorption (A), fluorescence emission (F) and phosphorescence emission (P) spectra of (a) 10 µM HSA and (b) 50 µM (*S*)-FBP. All samples were buffered with 0.01 M TRIS-HCl (pH 7.4). Absorption spectra were obtained in the absence of KI without deoxygenation. The fluorescence and phosphorescence spectra were recorded after addition of 0.2 M KI and deoxygenation using 2 mM Na_2SO_3.

The influence of ligand addition on the fluorescence spectra is minor but significant. The HSA fluorescence itself does not change upon addition of (*R*)-FBP (Figure 9.4a). The increase of the fluorescence observed at the short-wavelength side is due to the emission of the ligand after direct excitation. No FRET occurs since there is no spectral overlap between the Trp fluorescence emission and the singlet absorption of FBP (see Figure 9.3). The addition of (*S*)-FBP (Figure 9.4b), however, does slightly influence the HSA fluorescence. Binding of this enantiomer apparently changes the environment of Trp-214, which is in line with the phosphorescence results as will be discussed below. This is only observed at lower concentrations of ligand; at higher concentrations the HSA fluorescence does not change further and only an increasing ligand fluorescence is observed. Note that the increase in the ligand fluorescence is higher for (*R*)-FBP than for (*S*)-FBP. This indicates a possible difference in the fluorescence quantum yield and/or the excitation efficiency of the two FBP enantiomers after complexation with HSA.

In contrast to the minor effect on the HSA fluorescence, the addition of FBP causes a strong quenching of the HSA phosphorescence (Figures 9.4c and d). In order to investigate the quenching mechanism, the experiments were repeated using the amino acid L-Trp free in solution instead of HSA (Figure 9.4e). The phosphorescence emission of free L-Trp is almost completely quenched after addition of 10 µM (*S*)-FBP. Furthermore, the (*S*)-FBP phosphorescence intensity itself is much higher in the presence than in the absence of L-Trp, which is a clear indication of energy transfer from L-Trp to (*S*)-FBP. Similar results were observed for (*R*)-FBP, (*S*)-FBPMe and (*R*)-FBPMe with free L-Trp (data not shown).

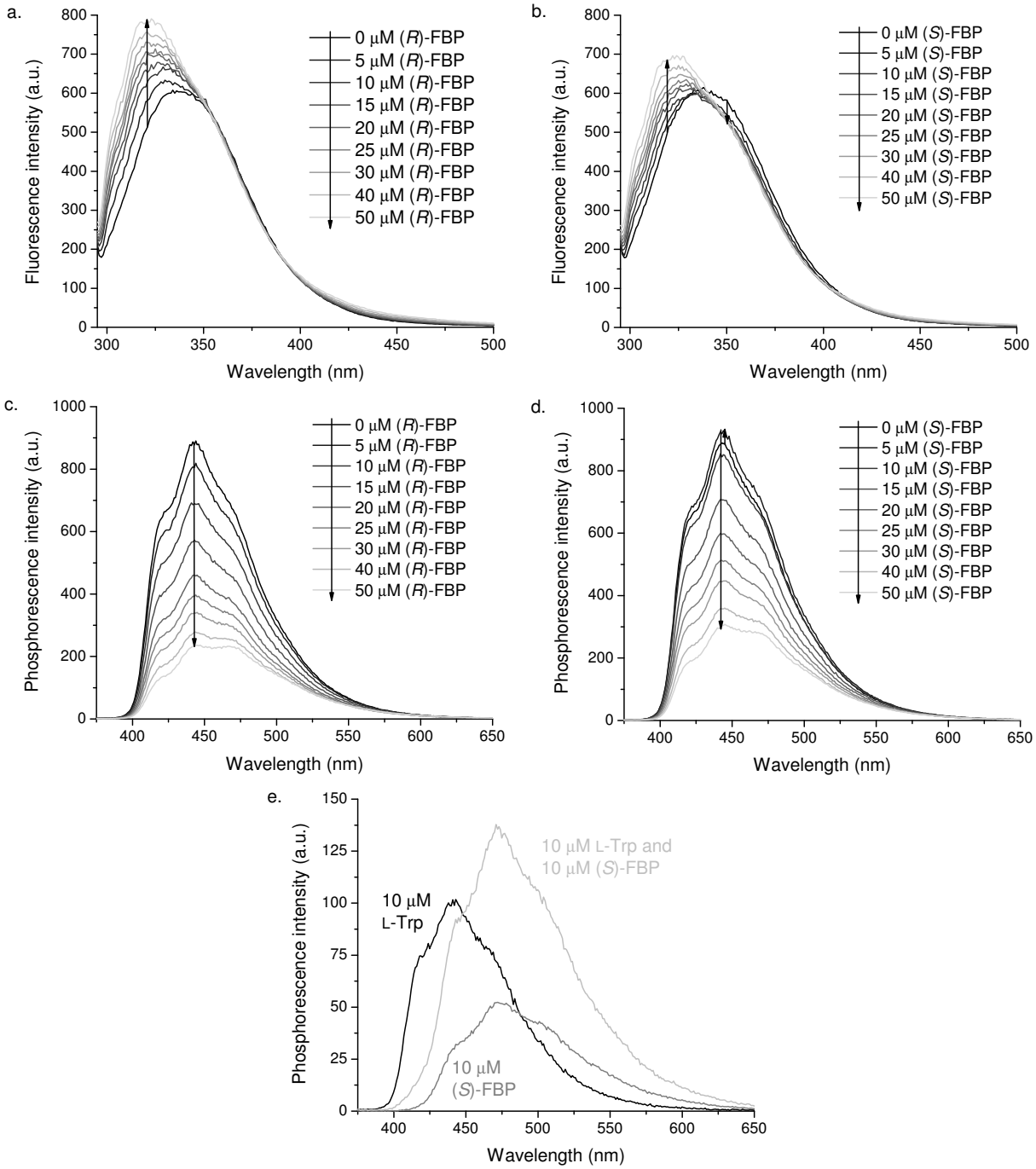

Figure 9.4: Fluorescence emission spectra of 10 μM HSA with increasing concentrations of (a) (*R*)-FBP and (b) (*S*)-FBP. Phosphorescence emission spectra of 10 μM HSA with increasing concentrations of (c) (*R*)-FBP and (d) (*S*)-FBP. (e) Phosphorescence emission spectra from samples of 10 μM L-Trp and/or 10 μM (*S*)-FBP. All samples were made in 0.01 M TRIS-HCl buffer (pH 7.4) with 0.2 M KI for enhanced intersystem crossing and 2 mM Na_2SO_3 for deoxygenation. Excitation was performed with a pulsed xenon lamp at 290 nm.

The much higher phosphorescence intensity of Trp-214 in HSA compared to the free amino acid L-Trp (compare Figures 9.4e with 9.4c and d) is mainly caused by difference in lifetime (τ_0 = 2.7 ms for HSA and τ_0 = 0.4 ms for L-Trp) and indicates the protection of this residue inside the protein matrix.[5] This protection makes the HSA phosphorescence quenching by FBP less efficient. In contrast to the complete quenching of the L-Trp phosphorescence, the HSA phosphorescence decreases only about 20% after the addition of 10 µM (*R*)-FBP (Figure 9.4c). There is a slight change in the peak shape due to the additional (*R*)-FBP phosphorescence at the red side of the spectrum (see also Figure 9.3), which becomes more obvious at higher ligand concentrations. In contrast to (*R*)-FBP, addition of low concentrations (*S*)-FBP (2.5 and 5 µM) causes a small increase in phosphorescence intensity of HSA (Figure 9.4d). This effect was also observed for other well-known and strong site II binders, including (*RS*)-ibuprofen, (*RS*)-naproxen, and octanoic acid (data not shown). In agreement with the fluorescence results of (*S*)-FBP and HSA as discussed above, this could indicate a change in environment of Trp-214. After this initial increase, the HSA phosphorescence intensity decreases with higher concentrations of (*S*)-FBP.

9.3.3 Stern-Volmer plots

The Stern-Volmer plots of the HSA phosphorescence quenching by FBP and FBPMe show similar trends for both the intensities and the lifetimes, which indicates a predominantly dynamic quenching mechanism. Static quenching plays only a minor role at higher ligand concentrations (data not shown). The dynamic quenching may be the result of diffusion-controlled collisions of free ligand with solvent exposed Trp-214. However, changes in lifetime may be observed as well if ligands bind at a distance of Trp-214 close enough to allow Dexter energy transfer at the timescale of phosphorescence. Furthermore, the flexibility of the HSA-ligand complexes may also play a role at the long timescales involved. The Stern-Volmer plots based on the longest HSA phosphorescence lifetime after bi-exponential fitting of the luminescence decay curves are shown in Figure 9.5 for the addition of (*R*)-FBP and (*S*)-FBP and their methyl esters. Emission was detected at 410 nm to prevent interference from the FBP phosphorescence.

Quenching of the phosphorescence of the free amino acid L-Trp starts immediately at low FBP concentrations (data not shown). The Stern-Volmer plots of the phosphorescence lifetime quenching of 10 µM HSA by FBP, however, show a distinctly non-linear behavior (Figure 9.5a). Little quenching is observed at low ligand concentrations, although based on reported binding constants most of the FBP should be complexed with HSA under these conditions.[30-32] Apparently, the distance between Trp-214 and bound FBP is too large for Dexter energy transfer to occur. At ligand concentrations above 10 µM the HSA phosphorescence quenching strongly increases. This stoichiometric ratio indicates that there is one high affinity binding site for FBP, which is known to be site II.[24,33]

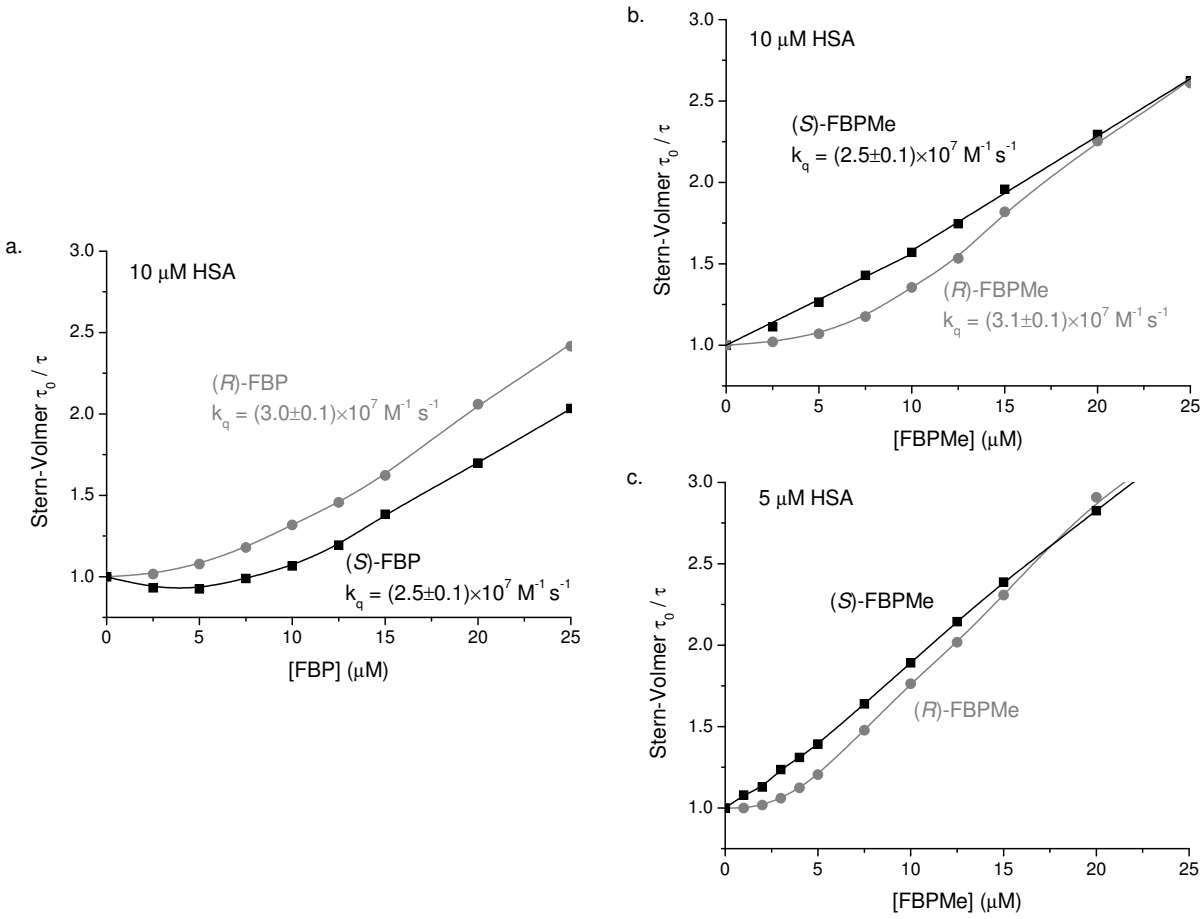

Figure 9.5: Stern-Volmer plots based on the longest HSA phosphorescence lifetime of (a) 10 μM HSA with increasing concentrations of (*S*)-FBP (■) and (*R*)-FBP (●), (b) 10 μM HSA with increasing concentrations of (*S*)-FBPMe (■) and (*R*)-FBPMe (●), and (c) 5 μM HSA with increasing concentrations of (*S*)-FBPMe (■) and (*R*)-FBPMe (●). All samples were made in 0.01 M TRIS-HCl (pH 7.4) with 0.2 M KI for enhanced intersystem crossing and 2 mM Na_2SO_3 for deoxygenation. Excitation was performed with a pulsed xenon lamp at 290 nm and emission was detected at 410 nm.

Flash photolysis experiments did not indicate a strong enantioselectivity in the binding of (*S*)-FBP and (*R*)-FBP to site I or II of HSA.[24] Interestingly, our phosphorescence measurements result in distinct Stern-Volmer plots for these enantiomers (Figure 9.5a). The phosphorescence lifetime of Trp-214 first increases at low (*S*)-FBP concentrations, which is not observed for (*R*)-FBP. Apparently, the complexation of (*S*)-FBP affects the direct environment of Trp-214 such that the triplet state of tryptophan is more protected. Unfortunately, a quantitative analysis of the Stern-Volmer plots is complicated by this change in lifetime since τ_0 is no longer fully identical to the HSA lifetime in the absence of free ligand. Using for τ_0 the lifetime at zero ligand concentration of 2.6 ms, the bimolecular rate constants related to the dynamic quenching at higher ligand levels are calculated to be $(2.5\pm0.1)\times10^7$ M^{-1} s^{-1} for (*S*)-FBP and $(3.0\pm0.1)\times10^7$ M^{-1} s^{-1} for (*R*)-FBP. This significant stereoselectivity indicates a lower accessibility of Trp-214 for free (*S*)-FBP than for free (*R*)-FBP.

The enantioselectivity given by the Stern-Volmer plots of the FBP methyl esters is very different from that of the carboxylic acids. Flash photolysis results[23,25] show that at low ligand:protein ratios no (*S*)-FBPMe or (*R*)-FBPMe is found free in solution, indicating a high association constant. The phosphorescence results in Figure 9.5b show a decrease in the Trp-214 phosphorescence lifetime starting directly at low added (*S*)-FBPMe concentrations with a minor increase in slope at ligand concentrations higher than 10 μM. Therefore, we conclude that (*S*)-FBPMe binds close enough to Trp-214 to cause Dexter energy transfer at the timescale of phosphorescence. No quenching of the HSA phosphorescence is observed at low (*R*)-FBPMe concentrations, which indicates that its distance to Trp-214 when bound is too large for Dexter energy transfer to occur. The large difference in triplet lifetimes of the methyl esters bound to site I obtained with the flash photolysis experiments (31.5 μs for (*S*)-FBPMe and 157.6 μs for (*R*)-FBPMe)[23,25] agrees with the observation that these two enantiomers have a distinct binding environment. The bimolecular rate constants for dynamic quenching of 10 μM HSA at high ligands levels are comparable to those of the corresponding anions: $(2.5\pm0.1)\times10^7$ M^{-1} s^{-1} for (*S*)-FBPMe and $(3.1\pm0.1)\times10^7$ M^{-1} s^{-1} for (*R*)-FBPMe based on τ_0 = 2.6 ms as found in absence of FBPMe. Apparently, at the timescale of these experiments, the methylation does not influence the accessibility of Trp-214 by the ligands from the bulk solution.

In order to ensure that the observed curves for FBPMe are not related to its low solubility in aqueous samples, Stern-Volmer plots were also measured at a lower protein concentration: Figure 9.5c shows the results for 5 μM HSA. Little difference is observed between the Stern-Volmer plots of 5 and 10 μM HSA for (*S*)-FBPMe; the quenching of the Trp-214 phosphorescence lifetime by (*S*)-FBPMe starts immediately at low ligand concentrations. The quenching by (*R*)-FBPMe, however, shows a clear dependence on the HSA concentration; the steep rise in the Stern-Volmer plots clearly starts at lower ligand concentration for the samples of 5 μM HSA.

Comparison of Figure 9.5a and 9.5b gives information about the influence of the methylation of the FBP enantiomers on the HSA phosphorescence quenching. Although the flash photolysis results indicated a clearly different distribution of (*R*)-FBP and (*R*)-FBPMe over site I and II,[23-25] the Stern-Volmer plots of these ligands are very similar. Apparently, the HSA binding of these ligands at either site does not cause quenching and phosphorescence cannot distinguish between them. Furthermore, the quenching constants of free (*R*)-FBP and (*R*)-FBPMe are similar, indicating that the accessibility of Trp-214 does not change significantly upon methylation of (*R*)-FBP. Also in the case of (*S*)-FBP, methylation does not influence the quenching constants. The Stern-Volmer plots of (*S*)-FBP and (*S*)-FBPMe, however, do differ significantly. Binding to site II of (*S*)-FBP causes a HSA lifetime increase at low concentrations, whereas binding of (*S*)-FBPMe to site I causes a decrease in the HSA lifetime at low concentrations.

9.4 Conclusions

Heavy-atom induced room-temperature phosphorescence is an appropriate tool for investigating the stereoselective binding of FBP enantiomers and their methyl esters to HSA. The HSA fluorescence is hardly influenced by these ligands; FRET does not occur since there is no spectral overlap between the HSA fluorescence and FBP or FBPMe absorption bands. In phosphorescence, however, clear phosphorescence quenching of Trp-214 is observed. Dexter energy transfer can be efficient if donor (Trp-214) and acceptor (FBP or FBPMe) are able to approach each other closely. Time-resolved measurements indicated that the quenching is predominantly dynamic of nature. A clear stereoselectivity is observed: The interaction of the FBP enantiomers en their methyl esters with HSA results in significantly different Stern-Volmer plots based on the longest lifetime of HSA; (*R*)-FBP quenches more than (*S*)-FBP, while for the methyl esters (*S*)-FBPMe quenches more than (*R*)-FBPMe. More investigation into the exact binding positions to HSA is needed for a more fundamental explanation of these influences and to combine the RTP and flash photolysis results appropriately. The difference in the dynamic quenching constants of the *S*-enantiomers and the *R*-enantiomers indicates a stereoselectivity in the accessibility of Trp-214, which is not influenced by the methylation.

References

(1) Cioni, P.; Strambini, G. B. *Biochim. Biophys. Acta* **2002**, *1595*, 116-130.

(2) Subramaniam, V.; Steel, D. G.; Gafni, A. In *Topics in fluorescence spectroscopy*, Volume 6: *Protein fluorescence*; Lakowicz, J. R. Ed.; Kluwer Academic/Plenum Publishers: New York, 2000.

(3) Vanderkooi, J. M. In *Topics in fluorescence spectroscopy*, Volume 3: *Biochemical applications*; Lakowicz, J. R. Ed.; Plenum Press: New York, 1992.

(4) Gonnelli, M.; Strambini, G. B. Biochim. *Biophys. Acta* **2009**, *1794*, 569-576.

(5) Gonnelli, M.; Strambini, G. B. *Biochemistry* **1995**, *34*, 13847-13857.

(6) Vanderkooi, J. M.; Calhoun, D. B.; Englander, S. W. *Science* **1987**, *236*, 568-569.

(7) Strambini, G. B. *Biophys. J.* **1987**, *52*, 23-28.

(8) Strambini, G. B.; Cioni, P. *J. Am. Chem. Soc.* **1999**, *121*, 8337-8344.

(9) Calhoun, D. B.; Englander, S. W.; Wright, W. W.; Vanderkooi, J. M. *Biochemistry* **1988**, *27*, 8466-8474.

(10) Calhoun, D. B.; Vanderkooi, J. M.; Englander, S. W. *Biochemistry* **1983**, *22*, 1533-1539.

(11) Strambini, G. B.; Gonnelli, M. *Biophys. J.* **2010**, *99*, 944-952.

(12) Dexter, D. L. *J. Chem. Phys.* **1953**, *21*, 836-850.

(13) Förster, T. *Discuss. Faraday Soc.* **1959**, 27, 7-17.

(14) Sudlow, G.; Birkett, D. J.; Wade, D. N. *Mol. Pharmacol.* **1975**, *11*, 824-832.

(15) Sudlow, G.; Birkett, D. J.; Wade, D. N. *Mol. Pharmacol.* **1976**, *12*, 1052-1061.

(16) Peters, T. *All about albumin: Biochemistry, genetics, and medical applications;* Academic Press: London, 1996.

(17) Chuang, V. T. G.; Otagiri, M. *Chirality* **2006**, *18*, 159-166.

(18) Wei, Y.; Dong, C.; Liu, D.; Shuang, S.; Huie, C. W. *Biomacromolecules* **2007**, *8*, 761-764.

(19) Davies, N. M. *Clin. Pharmacokin.* **1995**, *28*, 100-114.

(20) Hawkey, C. J. *Gastroenterology* **2000**, *119*, 521-535.

(21) Fukuhara, A.; Imai, T.; Otagiri, M. *Chirality* **1996**, *8*, 494-502.
(22) Mohan, R.; Ramaa, C. S. *Indian J. Chem.* **2007**, *40B*, 1164-1168.
(23) Jiménez, M. C.; Miranda, M. A.; Vayá, I. *J. Am. Chem. Soc.* **2005**, *127*, 10134-10135.
(24) Vayá, I.; Bueno, C. J.; Jiménez, M. C.; Miranda, M. A. *ChemMedChem* **2006**, *1*, 1015-1020.
(25) Vayá, I.; Jiménez, C.; Miranda, M. A. *J. Phys. Chem. B* **2008**, *112*, 2694-2699.
(26) Eftink, M. R.; Ghiron, C. A. *Anal. Biochem.* **1981**, *114*, 199-227.
(27) Lakowicz, J. R. *Principles of fluorescence spectroscopy*, 3rd ed.; Springer: New York, 2006.
(28) Cioni, P.; Gabellieri, M.; Gonnelli, M.; Strambini, G. B. *Biophys. Chem.* **1994**, *52*, 25-34.
(29) Schlyer, B. D.; Schauerte, J. A.; Steel, D. G.; Gafni, A. *Biophys. J.* **1994**, *67*, 1192-1202.
(30) Takla, P. G.; Schulman, S. G.; Perrin, J. H. *J. Phamaceut. Biomed.* **1985**, *3*, 41-50.
(31) Deschamps-Labat, L.; Péhourcq, F.; Jagou, M.; Bannwarth, B. *J. Pharmaceut. Biomed. Anal.* **1997**, *16*, 223-229.
(32) Wybranowski, T.; Cyrankiewicz, M.; Ziomkowska, B.; Kuszewski, S. *BioSystems* **2008**, *94*, 258-262.
(33) Rahman, M. H.; Yamasaki, K.; Shin, Y. H.; Lin, C. C.; Otagiri, M. *Biol. Pharm. Bull.* **1993**, *16*, 1169-1174.